Article

Neuron

Pheromones Modulate Learning by Regulating the Balanced Signals of Two Insulin-like Peptides

Highlights

- High population density suppresses learning of harmful food
- Balanced signals of two insulin-like peptides (ILPs) are critical for learning
- Pheromones during crowding disturb ILP signals by modulating ILP-producing neurons
- Pheromones increase consumption of harmful food and resistance to its pathogenicity

Authors

Taihong Wu, Fengyun Duan, Wenxing Yang, ..., QueeLim Ch'ng, Rebecca A. Butcher, Yun Zhang

Correspondence

yzhang@oeb.harvard.edu

In Brief

Wu et al. show that social signals of crowding inhibit worms from learning to avoid low-quality pathogenic food by disrupting balanced signals of two insulin-like peptides that are critical for learning to facilitate food intake when population density is high.

Wu et al., 2019, Neuron *104*, 1–15
December 18, 2019
https://doi.org/10.1016/j.neuron.2019.09.006

CellPress

Neuron
Article

Pheromones Modulate Learning by Regulating the Balanced Signals of Two Insulin-like Peptides

Taihong Wu,[1,2] Fengyun Duan,[1,2] Wenxing Yang,[1,2] He Liu,[1,2] Antonio Caballero,[3] Diana Andrea Fernandes de Abreu,[3] Abdul Rouf Dar,[4] Joy Alcedo,[5] QueeLim Ch'ng,[3] Rebecca A. Butcher,[4] and Yun Zhang[1,2,6,*]
[1]Department of Organismic and Evolutionary Biology, Harvard University, Cambridge, MA 02138, USA
[2]Center for Brain Science, Harvard University, Cambridge, MA 02138, USA
[3]Centre for Developmental Neurobiology, Institute of Psychiatry, Psychology and Neuroscience, King's College London, London SE1 1UL, UK
[4]Department of Chemistry, University of Florida, Gainesville, FL 32611, USA
[5]Department of Biological Sciences, Wayne State University, Detroit, MI 48202, USA
[6]Lead Contact
*Correspondence: yzhang@oeb.harvard.edu
https://doi.org/10.1016/j.neuron.2019.09.006

SUMMARY

Social environment modulates learning through unknown mechanisms. Here, we report that a pheromone mixture that signals overcrowding inhibits *C. elegans* from learning to avoid pathogenic bacteria. We find that learning depends on the balanced signaling of two insulin-like peptides (ILPs), INS-16 and INS-4, which act respectively in the pheromone-sensing neuron ADL and the bacteria-sensing neuron AWA. Pheromone exposure inhibits learning by disrupting this balance: it activates ADL and increases expression of *ins-16*, and this cellular effect reduces AWA activity and AWA-expressed *ins-4*. The activities of the sensory neurons are required for learning and the expression of the ILPs. Interestingly, pheromones also promote the ingestion of pathogenic bacteria while increasing resistance to the pathogen. Thus, the balance of the ILP signals integrates social information into the learning process as part of a coordinated adaptive response that allows consumption of harmful food during times of high population density.

INTRODUCTION

Various environmental contexts and the state of the nervous system can either promote or inhibit learning to generate adaptive values. Social information, such as the density of the conspecifics sharing the same habitat, represents one of the most important environmental conditions that impact survival. Previous studies on animals ranging from social insects to mammals show that social contexts or social experience modulate a wide range of behaviors, including learning and memory (Sokolowski, 2010). Although multiple sensory cues are used to communicate social information among individuals of the same species, pheromones have been found to modulate learning in both vertebrate and invertebrate animals (Bredy and Barad, 2008; Chabaud et al., 2009; Karlson and Luscher, 1959; Roberts et al., 2012; Vergoz et al., 2007). For example, a sex pheromone produced in the male mouse urine signals the presence of a male and potently promotes the learning of the location of the pheromone in both female and male mice. In contrast, one type of pheromone that is produced by the queen honeybee blocks the association of an odorant with electrical shocks in young worker bees (Karlson and Luscher, 1959; Roberts et al., 2012; Vergoz et al., 2007). In addition, the chemical signals contained in the sweat of stressed people alter the cognitive functions of the recipients (Chen et al., 2006). These earlier studies demonstrate profound modulation of learning by social context through transmission of pheromones and raise intriguing questions on the biological significance of the social modulation of learning. Meanwhile, the genes and neurons that integrate social signals with the regulation of learning remain largely unknown.

Insulin and insulin-like peptides (ILPs) regulate multiple physiological processes, including learning and memory, in both vertebrate and invertebrate animals by acting through highly conserved receptors and intracellular signaling pathways (Fernandez and Torres-Alemán, 2012; and the references therein). Previous studies in mammals and invertebrates have implicated insulin and ILPs in modulating brain functions in response to environmental cues, including food signals, to regulate behavior, particularly those important for seeking food, such as olfaction (Deijen et al., 1998; Marks et al., 2009; Root et al., 2011; Wu et al., 2005). Because insulin and ILPs are widely expressed in the nervous system, they often play critical roles in processing diverse sensory inputs (Aguado et al., 1994; Chen et al., 2013; Cornils et al., 2011; Li et al., 2003; Pierce et al., 2001; Ritter et al., 2013; Sandberg et al., 1988; Stylianopoulou et al., 1988; Tomioka et al., 2006). Because pheromones can signal population density, which is an important piece of social information critical for food availability, insulin and ILPs are candidate effectors of the pheromone-mediated modulation of olfactory learning.

In this study, we address the genes and neurons that integrate social information to modulate learning in *Caenorhabditis elegans* and characterize the underlying mechanisms by applying genetic and imaging tools to analyze the well-defined nervous system of the animal (Alcedo and Zhang, 2013; de Bono and Maricq, 2005; White et al., 1986). Small-molecule pheromones, including several ascarosides that can signal population density,

have been identified in the worms (Butcher et al., 2007; Jeong et al., 2005; Macosko et al., 2009; Srinivasan et al., 2008, 2012). These ascarosides regulate entry into dauer, an arrested larval stage in response to stress (Butcher et al., 2007; Jeong et al., 2005; Kim et al., 2009; McGrath et al., 2011), and modulate foraging, aggregation, repulsion, odorant-dependent dispersal and chemotaxis, stress response, and adult mating (Greene et al., 2016; Ludewig et al., 2013; Macosko et al., 2009; Srinivasan et al., 2012; Yamada et al., 2010). Using genetically encoded calcium reporters, previous studies show that pheromones evoke intracellular calcium transients in several sensory neurons. These sensory responses transmit the social information conveyed by the pheromones to the downstream circuit (Jang et al., 2012; Macosko et al., 2009; Ryu et al., 2018).

Previous studies show that *C. elegans* learns to reduce its preference for the smell of pathogenic bacteria, such as the *Pseudomonas aeruginosa* strain PA14 (Tan et al., 1999), after training with the pathogens (Zhang et al., 2005). This type of aversive olfactory learning depends on the virulence of the training pathogenic bacteria and resembles the Garcia's effect both in behavior and the regulatory signaling, through which animals learn to avoid the smell and/or taste of food that makes them ill (Garcia et al., 1955; Jin et al., 2016; Zhang et al., 2005). Here, we ask whether social environment of the worm regulates this form of learning. We show that a mixture of ascaroside pheromones that indicates high density of conspecifics or the cultivating medium conditioned by worms grown in high density inhibits the aversive learning of pathogenic bacteria. We demonstrate that learning to avoid PA14 depends on the balance of the activities of two ILPs, the ADL-expressed INS-16 and the AWA-expressed INS-4. Pheromone exposure disrupts the balance between the expression of *ins-4* and *ins-16* by upregulating *ins-16* in the pheromone-sensing neurons ADL, an effect that inhibits AWA-expressed *ins-4.* We also show that the pheromones regulate the sensory activities of ADL and AWA, which regulate both learning and ILP expression. Furthermore, we discover that pheromone exposure increases the ingestion of PA14 and enhances resistance to pathogen infection. Together, our findings elucidate the molecular and neuronal mechanisms that underlie the social influence on learning and show that ILPs integrate environmental context in the regulation of learning.

RESULTS

The Pheromone Mixture that Signals Overcrowding Inhibits Learning of Pathogenic Food

C. elegans learns to reduce its preference for the smell of pathogenic bacteria after training with the pathogen (Chen et al., 2013; Zhang et al., 2005). In this training paradigm, the animals on the training plate feed on PA14 after a small amount of the standard benign bacterium *E. coli* OP50 is consumed (Figures 1A and 1B). We use a modified chemotaxis assay on odorants (Bargmann et al., 1993) to measure the olfactory preference between a small lawn of PA14 and a small lawn of OP50 (Figure 1A; STAR Methods). This type of learning is contingent on the pathogenicity of the bacterium used for training and is reversible in adult animals (Ha et al., 2010; Zhang et al., 2005). Similar to previous studies, the naive adult animals did not display a strong preference between the smell of PA14 and the smell of OP50 (Figure 1C), but animals trained with PA14 avoided PA14, as indicated by a positive choice index (Figure 1C; STAR Methods). The difference between the choice index of the trained animals and the choice index of the naive animals generated the learning index. A positive learning index indicated the learned avoidance of PA14 (Figure 1D; STAR Methods).

Under our experimental conditions, PA14 is moderately virulent. The intestinal infection caused by ingesting PA14 causes a slow death of adult animals over a course of several days (Tan et al., 1999). Thus, compared with the standard worm food in the lab, the *E. coli* strain OP50, PA14 is a poor-quality and harmful food source. We asked whether social information modulated the aversive learning of PA14 in worms by adding the mixture of three synthetic ascarosides, ascr#2 (asc-C6-MK; C6), ascr#3 (asc-ΔC9; C9), and ascr#5 (asc-ωC3; C3), to the naive plate and the training plate at a final concentration of 1 μM for each ascaroside (Figure 1B; STAR Methods). Although the comparable concentration of the pheromones can induce dauer formation when food is scarce, the presence of food on the naive and the training plates prevented dauer formation. Meanwhile, the pheromone mixture signals a high worm population density in the environment (Butcher et al., 2007, 2008). We found that the pheromone mixture did not alter the preference between the OP50 odorants and the PA14 odorants in the naive animals (Figure 1C). However, the pheromones significantly weakened the avoidance of the PA14 odorants in the trained animals (Figure 1C), resulting in a complete loss of the aversive learning of PA14 (Figure 1D). In addition, worms that were mutated for *daf-22*, which encodes a peroxisome-associated thiolase required for the biosynthesis of ascarosides (Butcher et al., 2009), displayed a normal level of PA14 learning (Figure 1E), demonstrating that loss of the pheromones does not disrupt learning.

Because *C. elegans* secretes a complex mixture of pheromones that include C3, C6, and C9 (Butcher et al., 2007, 2008; Greene et al., 2016), we next examined whether the environmental cues generated by overcrowding similarly modulated the learning to avoid PA14. We grew worms in liquid culture in a high density for two generations and exposed the naive and the trained worms to the supernatants of the culture, which contained the pheromones secreted by the worms during high-density cultivation, as similarly described in Figures 1A and 1B. We found that, in comparison with the medium control (S medium in Figures 1F–1H), the culture supernatant of wild-type animals significantly decreased the choice index of the trained wild-type animals without altering the choice index of the naive wild-type, resulting in a loss of learning (Figures 1F–1H). In contrast, exposure to the culture supernatant of *daf-22* mutant animals did not alter the choice index of either naive or trained animals, producing a learning index comparable to that produced under the control condition (Figures 1F–1H). Together, our results demonstrate that the secreted pheromones that signal a high population density inhibit the aversive learning of a food source that harms *C. elegans.*

The AWA-Expressed *ins-4* and the ADL-Expressed *ins-16* Regulate Learning

Next, we sought the molecular and cellular mechanisms through which the pheromones modulate learning. In both vertebrates

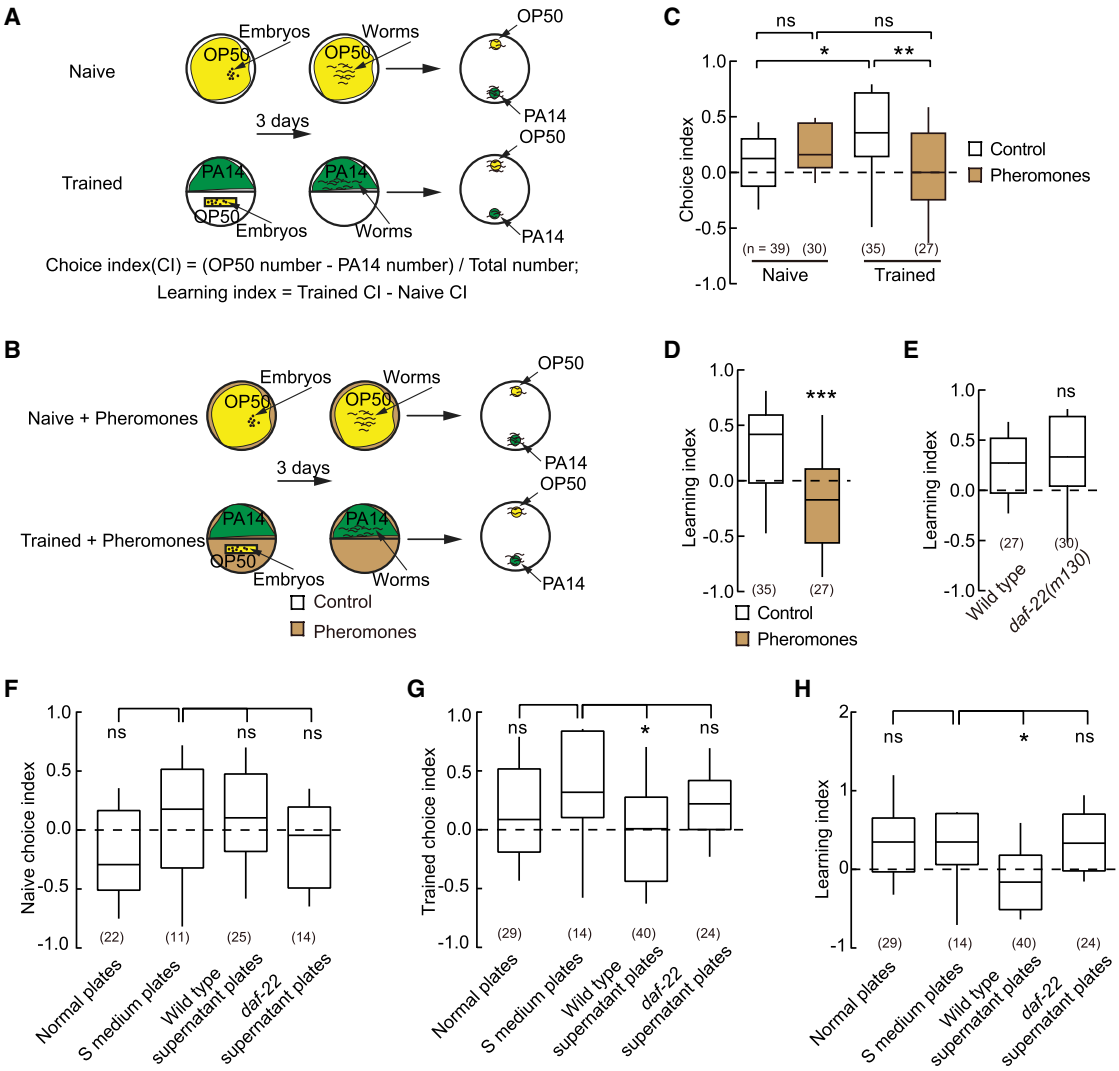

Figure 1. The Pheromone Mixture Signaling Crowding Inhibits Aversive Learning of Pathogenic Bacteria

(A and B) Schematic diagrams showing the training procedure and the assay for aversive olfactory learning of pathogenic bacterium *P. aeruginosa* PA14 without (A) or with (B) pheromone exposure.

(C) Wild-type naive animals do not strongly prefer the smell of PA14 or the smell of *E. coli* OP50, training with PA14 strongly reduces the preference for PA14; exposure to the pheromones does not alter the naive preference but disrupts the training-induced change in the preference of the trained animals. Two-way ANOVA with Tukey's multiple comparisons test.

(D) Wild-type learns to reduce their olfactory preference for PA14, and exposure to the pheromones abolishes learning. Student's t test.

(E) Mutating *daf-22* does not alter the aversive learning of PA14. Student's t test.

(F–H) Compared with the culture medium (S medium), exposure to the supernatant of a high-density culture of wild-type worms significantly reduces the trained choice index (G) without altering the naive choice index (F) of the wild-type animals, resulting in the loss of learning (H); in contrast, exposure to the supernatant of a high-density culture of *daf-22* mutant animals has no effect (F–H). One-way ANOVA with Dunnett's multiple comparisons test.

For (C)–(H), ***$p < 0.001$, **$p < 0.01$, and *$p < 0.05$; ns, not significant; the numbers of assays are shown in the parentheses. Boxes represent median and first and third quartiles, and whiskers represent 10th to 90th percentiles (generated using Igor Pro 6.12).

and invertebrates, ILPs regulate physiological events through highly conserved receptors and intracellular kinase cascades. Similar to *Drosophila* and humans, *C. elegans* expresses multiple ILPs that combinatorially regulate different physiological processes, including learning (Chen et al., 2013; Fernandes de Abreu et al., 2014; Fernandez and Torres-Alemán, 2012; Tomioka et al., 2006; and the references therein). Our previous studies show that the worm ILP pathway plays a critical role in the olfactory learning of pathogenic bacteria. Particularly, *ins-6* promotes learning by inhibiting *ins-7*, which antagonizes the function of the worm insulin-like growth factor receptor DAF-2 in the neural circuit that underlies pathogen learning (Chen et al., 2013; Ha et al., 2010). Here, we tested the mutations of several other ILP-encoding genes (Fernandes de Abreu et al., 2014). We found that individually mutating

several ILPs significantly disrupted the olfactory learning of PA14, and mutating a few others had no clear effect (Figure S1), which identifies the regulatory roles of several ILPs in learning. We focused on *ins-4* and *ins-16*, because deleting either *ins-6* or *ins-7* from the *ins-4* or the *ins-16* mutant animals did not alter the learning defect of the mutants (Figure S2). These results indicate that *ins-4* and *ins-16* do not require the function of *ins-6* or *ins-7* to regulate learning and likely regulate learning through a new pathway.

Expressing the genomic DNA that contained the 5′ and the 3′ regulatory regions and the coding region of *ins-4* or *ins-16* rescued the learning defect in the respective mutant animals (Figures 2A and 2B). These results indicate that INS-4 and INS-16 regulate the learning of PA14. To further characterize *ins-4* and *ins-16*, we examined the expression patterns of the two ILP-encoding genes using the transcriptional reporters in which the expression of the *mCherry*-encoding sequence was driven by the 5′ and 3′ regulatory sequences of *ins-4* or *ins-16.* We found the expression of the *ins-4* reporter in several neurons, including the sensory neurons AWA, ASI, and URX (Figures 2C and S3). We found the expression of the *ins-16* reporter in the sensory neuron ADL (Figure 2D). Expressing an *ins-4* coding sequence specifically in AWA fully rescued the learning defect in the *ins-4* deletion mutant animals (Figure 2A), and expressing the *ins-4* coding sequence in either ASI or URX did not rescue (Figure 2A). In addition, expressing an *ins-16* coding sequence specifically in ADL fully rescued the learning defect in the *ins-16* deletion mutant animals (Figure 2B). Together, these results demonstrate that *ins-4* expressed in the AWA sensory neurons and *ins-16* expressed in the ADL sensory neurons regulate the olfactory learning of PA14.

The Pheromones Signaling Overcrowding Modulate Learning by Regulating the Balance between INS-4 and INS-16 Signals

Intriguingly, although the loss of either *ins-4* or *ins-16* abolished the olfactory learning, deleting both *ins-4* and *ins-16* restored learning to the wild-type level (Figures 2E and S2), suggesting that the balance between these two ILP signals are critical for olfactory learning. Previously, we showed that mutating the worm insulin-like growth factor receptor *daf-2* disrupted the aversive learning of PA14 (Chen et al., 2013). Here, we found that mutating *daf-2* in either the *ins-4* or the *ins-16* single mutants or in the *ins-4; ins-16* double mutants abolished the olfactory learning, consistent with *daf-2* being downstream of the ILPs that regulate learning (Figures 2F and S2). Next, we tested the possibility that the balance between the *ins-4* and the *ins-16* signals is critical for the aversive olfactory learning. We used the miniMos technique (Frøkjær-Jensen et al., 2014) to generate transgenic animals that expressed a defined copy number of the two transgenes, the AWA-expressed *ins-4* that rescued the learning defect in the *ins-4* mutants (Figure 2A) and the ADL-expressed *ins-16* that rescued the learning defect in the *ins-16* mutants (Figure 2B). First, we expressed either two copies of the AWA-expressed *ins-4* or two copies of the ADL-expressed *ins-16* in the *ins-4; ins-16* double mutants. We found that, although the *ins-4; ins-16* double mutants were normal in learning (Figure 2E), expressing only *ins-4* in AWA or only *ins-16* in ADL disrupted learning (Figure 3A). Next, we used the same transgenes to express two additional copies of the AWA-expressed *ins-4* or two additional copies of the ADL-expressed *ins-16* in wild-type animals. We found that overexpressing either of the transgenes also disrupted learning (Figure 3A), indicating that a relatively higher level of either the AWA-expressed *ins-4* or the ADL-expressed *ins-16* is similarly detrimental for learning. Furthermore, we found that the transgenic animals expressing four copies of both transgenes were normal in learning (Figure 3A), indicating that the balanced expression of a higher level of *ins-4* and *ins-16* is also sufficient for normal learning. Together, by testing combinations of 0, 2, or 4 copies of these two ILPs, we demonstrate that the balance between the INS-4 signal produced by AWA and the INS-16 signal produced by ADL is critical for the olfactory learning of PA14.

Intriguingly, by quantifying the intensity of the *ins-4p::mCherry* and the *ins-16p::mCherry* signals, we found that exposure to the pheromones differentially altered the expression of *ins-4* and *ins-16*. We found that exposure to the pheromones significantly decreased the expression of *ins-4* in AWA and significantly increased the expression of *ins-16* in ADL in naive animals (Figures 3B and 3C), disrupting the balance between these two ILP signals. Similarly, although training with PA14 increased both the expression of *ins-4* in AWA and the expression of *ins-16* in ADL, pheromone exposure antagonized the training effect on the AWA-expressed *ins-4* by decreasing the expression back to the naive level but further increased the ADL-expressed *ins-16* (Figures 3B and 3C). Thus, pheromone exposure also disrupts the balance between the AWA-expressed *ins-4* and the ADL-expressed *ins-16* in trained animals. In comparison, pheromone exposure did not alter the expression of *ins-4p::mCherry* in either ASI or URX in naive animals or significantly antagonized the training-induced expression of the reporter in these neurons (Figures 3D and 3E). Together, these results show that the pheromones inhibit learning by disturbing the balance of the two ILPs that is critical for learning.

To further characterize this mechanism that underlies the modulation of learning by the pheromones, we tested the hypothesis that resetting the balance between the AWA-expressed *ins-4* and the ADL-expressed *ins-16* should restore learning. First, we found that, although pheromone exposure abolished learning in the wild-type animals, it had no effect on the *ins-4; ins-16* double mutant animals (Figure 3F), indicating that the pheromones modulate learning by regulating *ins-4* and *ins-16*. Second, we found that pheromone exposure, which downregulated the *ins-4* expression in AWA and upregulated the *ins-16* expression in ADL, rescued the learning defect in the *ins-16* deletion mutant animals, but not the learning defect in the *ins-4* deletion mutants (Figure 3F). Together, these results again demonstrate that the pheromone signals modulate the learning of the harmful food PA14 by regulating a balance between the expression of *ins-4* in AWA and the expression of *ins-16* in ADL.

We next tested the possibility that regulating the balance between the expression of *ins-4* in AWA and the expression of *ins-16* in ADL serves as a general mechanism to integrate environmental conditions into the regulation of learning. The concentration of salt, i.e., NaCl, in the standard *C. elegans* cultivating condition is around 50 mM (Brenner, 1974), and

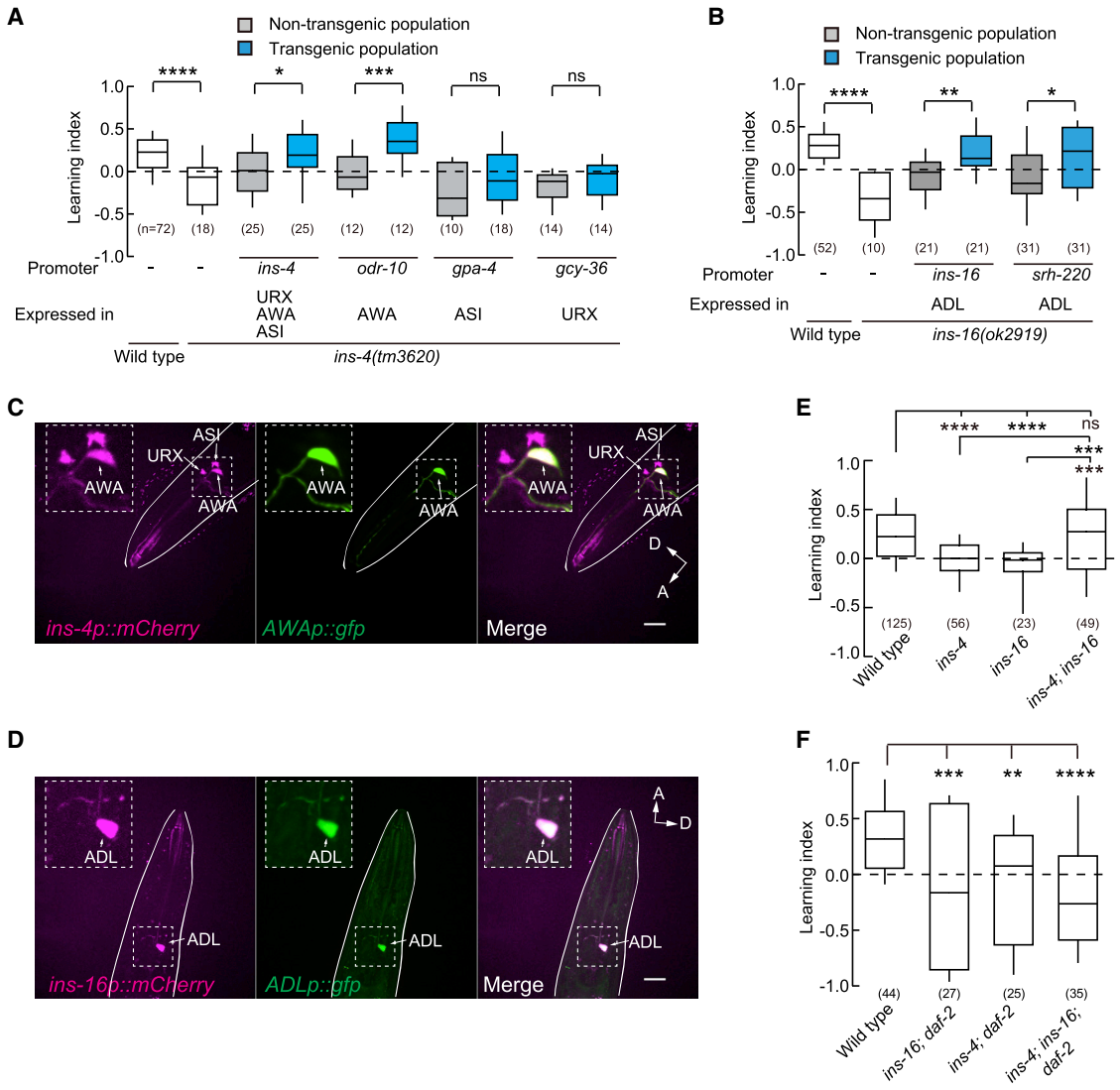

Figure 2. AWA-Expressed *ins-4* and ADL-Expressed *ins-16* Regulate the Learning of PA14

(A) Deleting *ins-4* disrupts the learning of PA14, and expressing a wild-type *ins-4* genomic DNA sequence or a wild-type *ins-4* coding sequence in the sensory neuron AWA rescues the learning defect; but the expression in ASI or URX does not rescue. Student's t test and Mann-Whitney U test were used to compare wild-type with mutant or transgenic animals with non-transgenic controls.

(B) Deleting *ins-16* disrupts the learning of PA14, and expressing a wild-type *ins-16* genomic DNA sequence or a wild-type *ins-16* coding sequence in the sensory neuron ADL rescues the learning defect. Student's t test and Mann-Whitney U test were used to compare wild-type with mutant or transgenic animals with non-transgenic controls.

(C and D) The transcriptional reporter *ins-4p::mCherry* is expressed in sensory neurons, including AWA (C), and *ins-16p::mCherry* is expressed in sensory neuron ADL (D). (C) shows individual and merged images of *ins-4p::mCherry* (magenta) and *AWAp::gfp* (green), and (D) shows individual and merged images of *ins-16p::mCherry* (magenta) and *ADLp::gfp* (green). Small panels show enlarged views of the neurons. Scale bars, 20 μm. The shape of the worm is outlined, A, anterior; D, dorsal.

(E) Although deleting either *ins-4* or *ins-16* abolishes the learning of PA14, deleting both restores learning to the wild-type level. One-way ANOVA with Tukey's multiple comparisons test.

(F) The double-mutant animals *ins-4; daf-2* and *ins-16; daf-2* and the triple mutant animals *ins-4; ins-16; daf-2* are defective in learning. One-way ANOVA with Dunnett's multiple comparisons test.

For (A), (B), (E), and (F), ****$p < 0.0001$, ***$p < 0.001$, **$p < 0.01$, and *$p < 0.05$; ns, not significant; the numbers of assays are shown in the parentheses. Boxes represent median and first and third quartiles, and whiskers represent 10th to 90th percentiles (generated using Igor Pro 6.12).

See also Figures S1, S2, and S3.

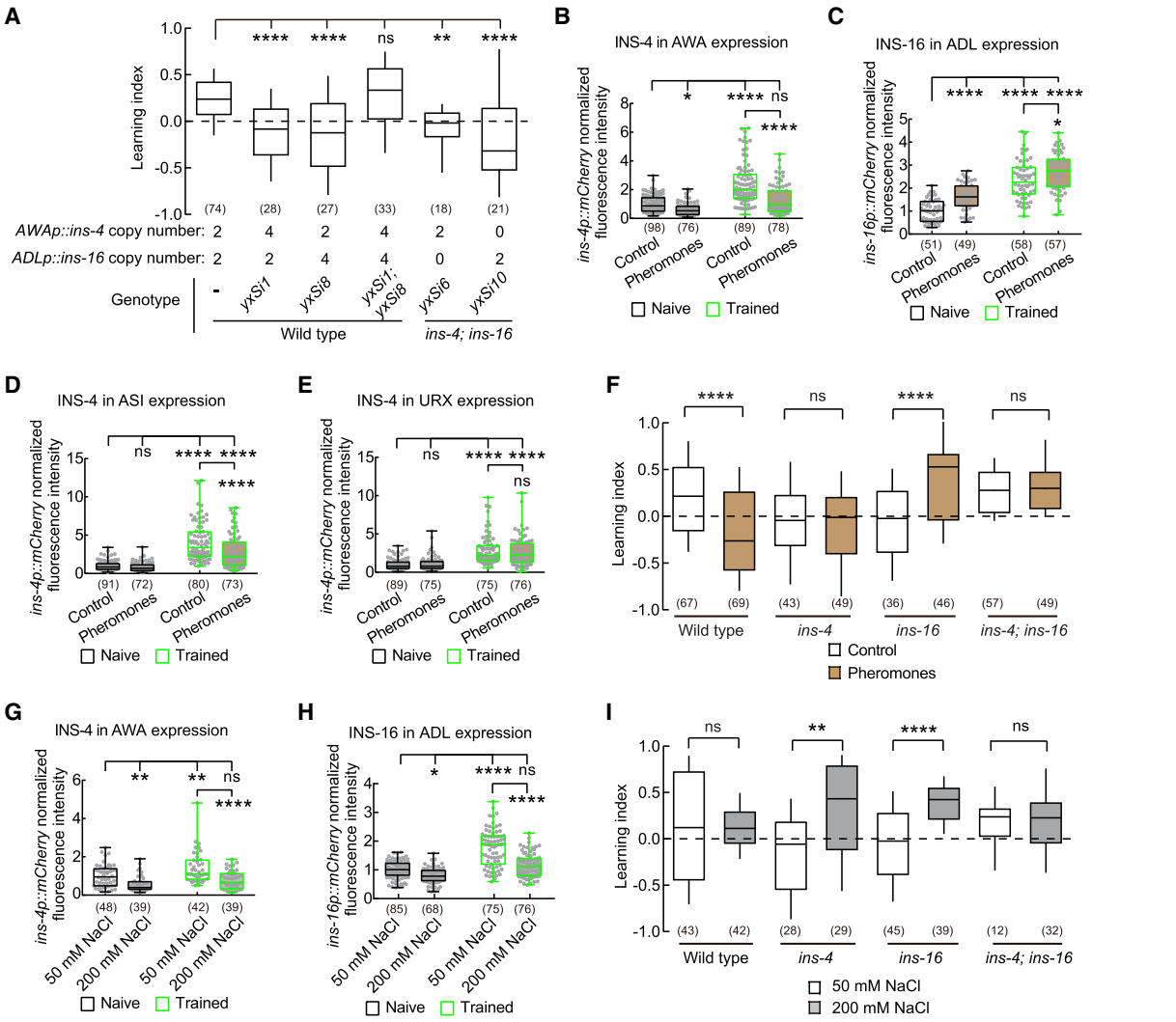

Figure 3. The Pheromones and High-Salt Condition Modulate the Learning of PA14 by Regulating the Balance between INS-4 and INS-16

(A) Expressing two copies of AWA-expressed *ins-4* or two copies of ADL-expressed *ins-16* in the *ins-4; ins-16* double mutants disrupts the learning of PA14, and expressing two additional copies of AWA-expressed *ins-4* or two additional copies of ADL-expressed *ins-16* in the wild-type animals also disrupts learning; however, expressing four copies of AWA-expressed *ins-4* and four copies of ADL-expressed *ins-16* generates normal learning. Boxes represent median and first and third quartiles, and whiskers represent 10th to 90th percentiles (generated using Igor Pro 6.12). The numbers of assays are shown in the parentheses. One-way ANOVA with Dunnett's multiple comparisons test.

(B and C) Training with PA14 increases the expression of *ins-4* in AWA, and pheromone exposure decreases the expression of *ins-4* in AWA in both naive and trained animals (B); in contrast, training with PA14 and pheromone exposure both increase the expression of *ins-16* in ADL (C).

(D and E) The effects of training and pheromone exposure on *ins-4* expression in ASI (D) or URX (E).

(F) The pheromones inhibit the learning of PA14 in wild-type and rescue the learning defect in the *ins-16* deletion mutant animals without altering learning of the *ins-4* mutant animals or the *ins-4; ins-16* double-mutant animals. Boxes represent median and first and third quartiles, and whiskers represent 10th to 90th percentiles (generated using Igor Pro 6.12). The numbers of assays are shown in the parentheses. Student's t test and Mann-Whitney U test.

(G and H) Training with PA14 increases the level of AWA-expressed *ins-4* (G) and the level of ADL-expressed *ins-16* (H), and exposure to high salt (200 mM NaCl) decreases the expression of *ins-4* in AWA (G) and the expression of *ins-16* in ADL (H). The fluorescence intensity of individual neurons is normalized by the average fluorescence intensity of the neurons of the naive animals grown at 50 mM NaCl. Boxes show the median and first and third quartiles, and whiskers show the minimum and the maximum (GraphPad Prism 8). The numbers of the neurons quantified are shown in the parentheses, and individual data points are shown as dots. One-way ANOVA with Tukey's multiple comparisons test.

(I) Exposure to high salt (200 mM NaCl) rescues the learning defect of *ins-4* mutant animals and *ins-16* mutant animals without altering learning in either wild-type animals or *ins-4; ins-16* double-mutant animals. Boxes represent median and first and third quartiles, and whiskers represent 10th to 90th percentiles (generated using Igor Pro 6.12). The numbers of assays are shown in the parentheses. Student's t test and Mann-Whitney U test.

For (B)–(E), the fluorescence intensity of individual neurons is normalized by the average fluorescence intensity of the neurons of the naive control animals; boxes show the median and first and third quartiles, and whiskers show the minimum and the maximum (GraphPad Prism 8). The numbers of

(legend continued on next page)

the worm is able to distinguish a wide range of salt concentrations (Luo et al., 2014). We found that exposure to 200 mM salt decreased the expression of *ins-4* in AWA and the expression of *ins-16* in ADL in both naive and trained animals, thereby maintaining the balance between the two ILPs (Figures 3G, 3H, and S4). Consistent with our hypothesis, we found that wild-type animals learned to avoid PA14 similarly in the presence of 200 mM or 50 mM salt condition (Figure 3I). Strikingly, exposure to 200 mM salt concentration rescued the learning defects in both the *ins-4* mutant animals and the *ins-16* mutant animals but had no effect on the learning of the *ins-4; ins-16* double mutant animals (Figure 3I). This further supports our hypothesis by showing that rescuing the balance between the AWA-expressed INS-4 and the ADL-expressed INS-16 with high salt allows the single mutant animals to learn. These results also demonstrate that regulating the relative expression of *ins-4* in AWA and *ins-16* in ADL is a general mechanism through which the environment modulates learning.

The Pheromones Modulate the Neuronal Activities of ADL and AWA, which Are Critically Required for Learning

Next, we asked how the pheromones interacted with the ILP-producing sensory neurons AWA and ADL. We performed *in vivo* calcium imaging to examine the activities of these sensory neurons in response to the pheromones and the bacterial food using transgenic animals that expressed the genetically encoded calcium-sensitive reporter GCaMP6s in AWA or GCaMP3 in ADL (Ryu et al., 2018). We performed the imaging experiments in a microfluidic device (Chronis et al., 2007), where sensory stimuli were delivered to the GCaMP-expressing transgenic animal that was confined within the device and had limited movement during the recording. Previous studies show that stimulating the animals with ascr#3 activates ADL, as indicated by an increase in the intracellular GCaMP signal upon exposure to ascr#3 (Jang et al., 2012; Ryu et al., 2018). Here, we found that the mixture of ascr#2, ascr#3, and ascr#5 also activated ADL in naive animals but to a much lesser extent in PA14-trained animals (Figures 4A and 4B). Prior pheromone exposure reduced the response of ADL and abolished the difference in the ADL response of naive and PA14-trained animals (Figures 4A and 4B). In contrast, AWA did not respond to the pheromone mixture (Figures 4C and 4D).

Next, we stimulated AWA and ADL with the medium that was conditioned by OP50 or PA14 (STAR Methods). Previous studies show that AWA, but not ADL, responds to *E. coli* OP50 (Zaslaver et al., 2015). We found that ADL did not respond to either of the food-conditioned media, regardless of prior pheromone treatment (Figures 4E and 4F). In comparison, switching from OP50 to PA14 evoked a strong increase in the AWA-expressed GCaMP6 signal in naive animals (Figures 4G and 4H). AWA mediates the attractive response to several odorants, and exposure to these odorants activates AWA, as demonstrated by increased GCaMP signals in AWA (Larsch et al., 2015). Thus, AWA responds to the PA14-conditioned medium as more attractive than the OP50-conditioned medium in naive animals. Training with PA14 reversed the AWA responses to the bacteria-conditioned media, resulting in decreased calcium transients in response to the switch from the OP50-conditioned medium to the PA14-conditioned medium and increased calcium transients upon the switch from PA14 to OP50 (Figures 4G and 4H). These results indicate that, in trained animals, AWA now responds to OP50 as the more attractive cue than PA14.

Pheromone exposure suppressed the PA14-evoked calcium transients in AWA in naive animals without further changing the responses of AWA to the bacteria-conditioned media in trained animals (Figures 4G and 4H). Hence, pheromone exposure also significantly reduced the difference in food-evoked AWA activities of naive and trained animals, which is consistent with the inhibitory effect of the pheromones on the learning of PA14 avoidance. Together, these results indicate that pheromone exposure modulates the training-induced difference in the neuronal response of ADL to the pheromones and the neuronal response of AWA to the bacterial odorants between naive and trained animals, the latter of which, together with other training-dependent changes (Chen et al., 2013; Jin et al., 2016; Liu et al., 2018), underlies the reduced preference for the training pathogen in trained animals.

Next, we asked whether the neuronal activities of ADL and AWA were important for learning. We expressed a histamine-gated chloride channel (HisCl1) selectively in ADL or AWA. The *C. elegans* genome does not encode any histamine-gated chloride channel, and ectopical expression of HisCl1 inhibits the activity of the expressing neurons in the presence of histamine (Pokala et al., 2014). We found that histamine treatment of the animals that express HisCl1 in ADL or AWA during training, during choice test, or during training and choice test completely disrupted the learning of PA14 (Figures 4I and 4J). These results indicate that the neuronal activities of ADL and AWA are critical for the worms to generate and display the learning of PA14 and that pheromone exposure, which inhibits learning, alters the sensory responses of these neurons.

ins-16 in the Pheromone-Sensing Neuron ADL Inhibits AWA-Expressed *ins-4* and AWA Activity

We have shown that pheromone exposure inhibits learning by disturbing the balance between the AWA-expressed *ins-4* and the ADL-expressed *ins-16.* Although ADL responds to the pheromones, AWA does not. Thus, we asked how pheromone exposure regulated the expression of *ins-4*. Interestingly, we found that deleting *ins-16* significantly increased the expression of *ins-4* in AWA, indicating that *ins-16* suppresses *ins-4* expression (Figure 5A). Because pheromone exposure increases the expression of *ins-16* in ADL (Figure 3C), we next asked whether

the neurons quantified are shown in the parentheses, and individual data points are shown as dots. One-way ANOVA with Tukey's multiple comparisons test.

For all, ****$p < 0.0001$, ***$p < 0.001$, **$p < 0.01$, and *$p < 0.05$; ns, not significant.

See also Figure S4.

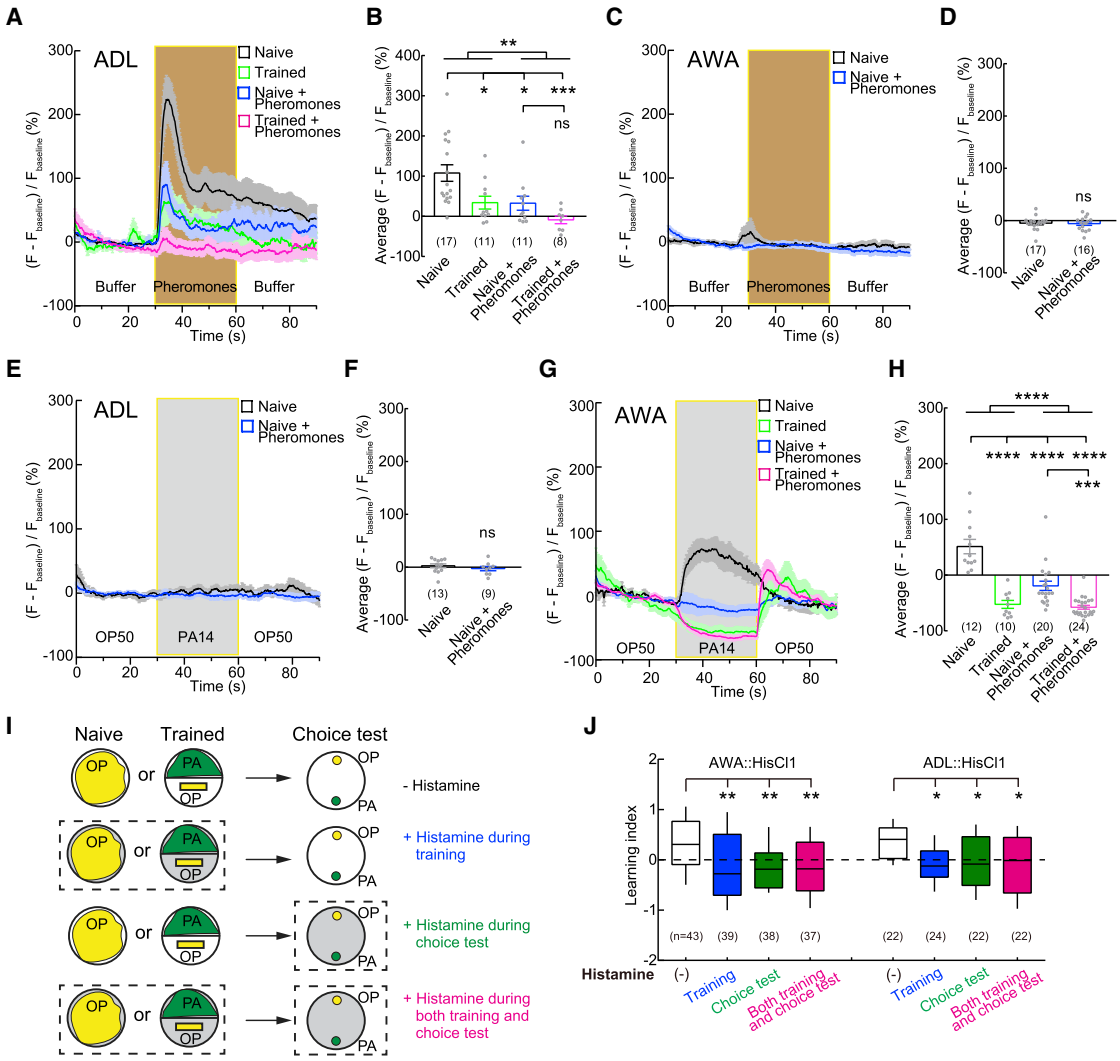

Figure 4. Training and Pheromone Exposure Regulate the Neural Activities of ADL and AWA, Both of Which Are Required for Learning

(A–D) The GCaMP signal in ADL increases in response to the stimulation of the pheromones, which is decreased by training and pheromone exposure (A and B), but the GCaMP signal in AWA does not respond to the pheromones (C and D). *F* is the fluorescence intensity of the neuron at each time point subtracted by the background signal, and $F_{baseline}$ is the average fluorescence intensity during the 30-s window before the pheromone stimulation. The solid lines and the shades in (A) and (C) are mean responses and SEM of multiple animals, respectively; the bar graphs in (B) and (D) show the quantitation of the average $(F - F_{baseline})/F_{baseline}$ (%) during the pheromone stimulation, mean ± SEM (generated using Igor Pro 6.12), the numbers of the transgenic animals measured are in the parentheses, and individual data points are shown as dots. Two-way ANOVA with Tukey's multiple comparisons test (B) and Mann-Whitney U test (D).

(E–H) The GCaMP signal in ADL does not respond to the OP50-conditioned medium or the PA14-conditioned medium (E and F), but the GCaMP signal in AWA increases in response to the switch from the OP50-conditioned medium to the PA14-conditioned medium, which is modulated by training and pheromone exposure (G and H). *F* is the fluorescence intensity of the neuron at each time point subtracted by the background signal, and $F_{baseline}$ is the average fluorescence intensity during the 30-s window before the PA14 stimulation. The solid lines and the shades in (E) and (G) are mean responses and SEM of multiple animals, respectively; the bar graphs in (F) and (H) show the quantitation of the average $(F - F_{baseline})/F_{baseline}$ (%) during the PA14 stimulation, mean ± SEM (generated using Igor Pro 6.12), the numbers of the transgenic animals measured are in the parentheses, and individual data points are shown as dots. Student's t test (F) and two-way ANOVA with Tukey's multiple comparisons test (H).

(I and J) Inhibiting AWA or ADL by treating the transgenic animals respectively expressing HisCl1 in AWA or ADL with histamine during training, during choice test, or during training and choice test, as shown in (I), disrupts learning (J). One-way ANOVA with Dunnett's multiple comparisons test. Boxes represent median and first and third quartiles, and whiskers represent 10th to 90th percentiles (generated using Igor Pro 6.12). The numbers of the assays are in the parentheses. In (I), OP denotes OP50 and PA denotes PA14.

For (A)–(H) and (J), ****p < 0.0001, ***p < 0.001, **p < 0.01, and *p < 0.05; ns, not significant.

overexpressing *ins-16* mimicked the pheromone effect of reducing *ins-4* expression in AWA. Increasing the copy number of *ins-16* in ADL in the wild-type background (*yxSi8* in Figure 5B) significantly decreased *ins-4* expression in AWA, an effect similar to that of pheromone exposure (Figure 5B). Next, we asked whether *ins-16* was the only factor that mediated the

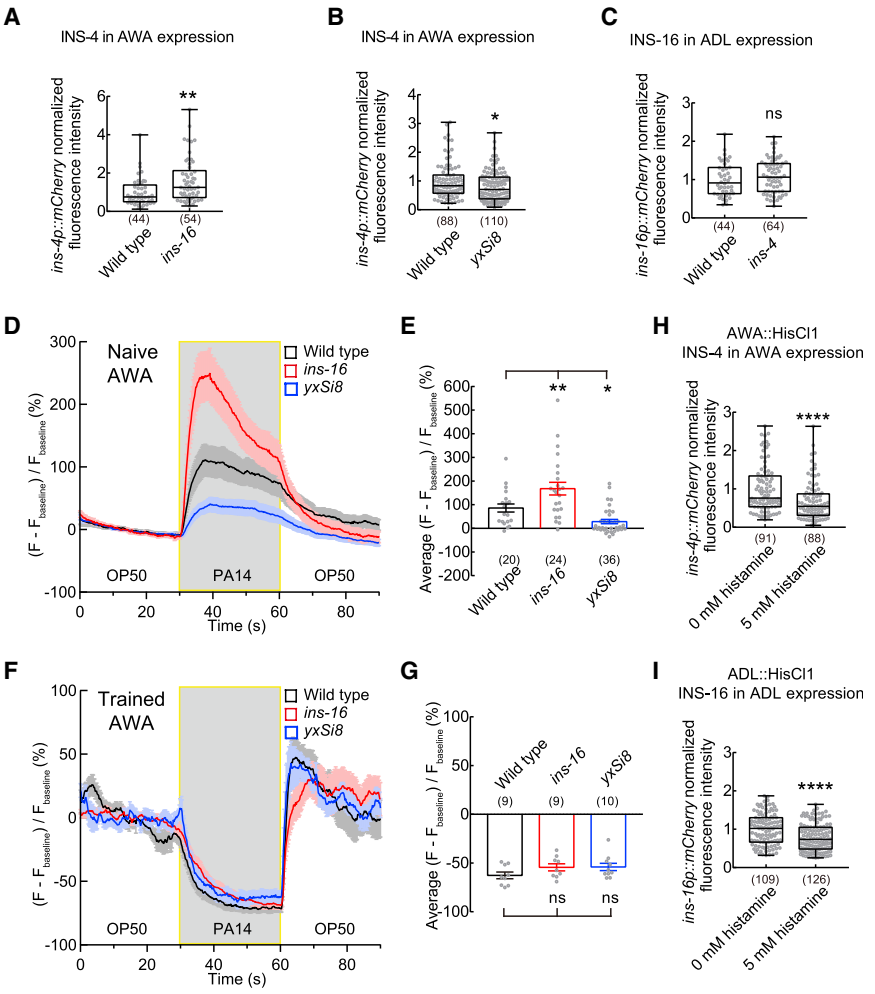

Figure 5. *ins-16* Regulates AWA Neural Activity and Its Expression of *ins-4*

(A and B) Deleting *ins-16* (A) or increasing the copy number of *ins-16* (B; *yxSi8*), respectively, increases or decreases the expression of *ins-4* in AWA. Mann-Whitney U test.

(C) Deleting *ins-4* does not alter the expression of *ins-16* in ADL. Student's t test.

(D–G) Deleting *ins-16* or increasing the copy number of *ins-16* (*yxSi8*), respectively, increases or decreases the GCaMP6 signal in AWA evoked by switching from OP50-conditioned medium to PA14-conditioned medium in naive animals (D and E), and they have no effect in the trained animals (F and G). *F* is the fluorescence intensity of the neuron at each time point subtracted by the background signal, and $F_{baseline}$ is the average fluorescence intensity during the 30-s window before the PA14 stimulation; the solid lines and the shades in (D) and (F) are mean responses and SEM of multiple animals, respectively, and the bar graphs in (E) and (G) show the quantitation of the average $(F - F_{baseline})/F_{baseline}$ (%) during PA14 stimulation, mean ± SEM (generated using Igor Pro 6.12), the numbers of the transgenic animals measured are in the parentheses, and individual data points are shown as dots. In (E) and (G), one-way ANOVA with Dunnett's multiple comparisons test was used.

(H and I) Inhibiting AWA by treating the transgenic animals expressing HisCl1 in AWA with histamine strongly decreases the expression of *ins-4* in AWA (H), and inhibiting ADL by treating the transgenic animals expressing HisCl1 in ADL with histamine decreases the expression of *ins-16* in ADL (I). Mann-Whitney U test.

For (A)–(C), (H), and (I), the fluorescence intensity of individual neurons is normalized by the average fluorescence intensity of the neurons of the wild-type animals or the control animals; boxes show the median and first and third quartiles, and whiskers show the minimum and the maximum (GraphPad Prism 8). The numbers of the neurons quantified are shown in the parentheses, and individual data points are shown as dots.

For all, ****p < 0.0001, ***p < 0.001, **p < 0.01, and *p < 0.05; ns, not significant.

See also Figure S5.

modulation of *ins-4* by the pheromones. We found that, in the *ins-16* deletion mutant animals, pheromone exposure continued to suppress AWA-expressed *ins-4* in both naive and trained animals (Figure S5), indicating that other factors also mediate pheromone-dependent suppression of *ins-4* expression when *ins-16* is deleted. In contrast, deleting *ins-4* does not alter the expression of *ins-16* (Figure 5C). Together, these results indicate that pheromone exposure activates ADL and stimulates its expression of *ins-16* and that increasing *ins-16* inhibits AWA-expressed *ins-4*. This regulatory cascade serves as one mechanism through which the social pheromones perturb the balance between *ins-16* and *ins-4* to block learning.

Similarly, we asked how pheromones modulated AWA sensory response to food odorants, because AWA does not respond to the pheromones. We found that deleting *ins-16* strongly increased the AWA GCaMP signals evoked by the PA14-conditioned medium, revealing an *ins-16*-dependent inhibitory effect on the AWA sensory response (Figures 5D and 5E). Consistent with this idea, overexpressing *ins-16* from ADL in wild-type, i.e., *yxSi8*, suppressed the AWA sensory response to the switch from the OP50-conditioned medium to the PA14-conditioned medium in naive animals, mimicking pheromone exposure (Figures 4G, 4H, 5D, and 5E). In addition, this ADL overexpression of *ins-16* did not change the AWA response to the food-conditioned media in trained animals (Figures 5F and 5G), again similar to the pheromone effect on the sensory responses of AWA in trained animals (Figures 4G and 4H). Thus, the pheromones increase *ins-16* expression in the pheromone-sensing neurons ADL, and increasing *ins-16* expression modulates AWA sensory response.

We further characterized whether the activities of the sensory neurons ADL and AWA were important for their respective expression of *ins-16* and *ins-4.* We measured the intensity of the transcriptional reporter for *ins-16* or *ins-4* in animals that express the histamine-gated chloride channel HisCl1 in ADL or AWA, respectively. We found that the inhibition of ADL or

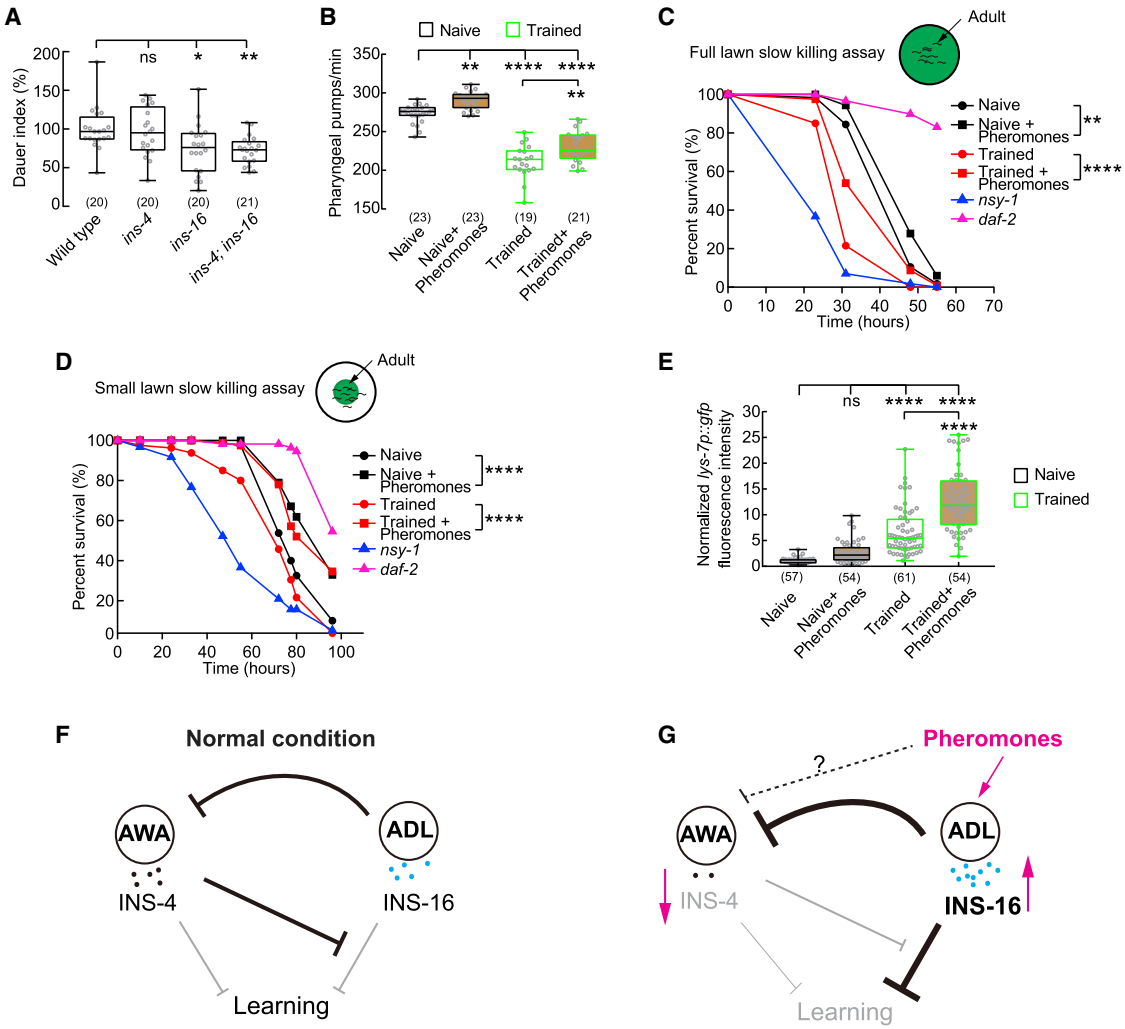

Figure 6. Pheromone Exposure Increases Feeding and Enhances Immune Resistance

(A) The *ins-16* mutant animals and the *ins-4; ins-16* double-mutant animals are defective in dauer formation (STAR Methods). One-way ANOVA with Dunnett's multiple comparisons test. The numbers of assays are shown in the parentheses, and individual data points are shown as dots. Boxes show the median and first and third quartiles, and whiskers show the minimum and the maximum (GraphPad Prism 8).

(B) Training with PA14 decreases pumping rate, and pheromone exposure increases the pumping rate in both naive and trained animals (STAR Methods). One-way ANOVA with Tukey's multiple comparisons test. The numbers of animals measured are shown in the parentheses, and individual data points are shown as dots. Boxes show the median and first and third quartiles, and whiskers show the minimum and the maximum (GraphPad Prism 8).

(C and D) Pheromone exposure enhances the resistance to PA14 in naive and PA14-trained wild-type animals in the full-lawn slow killing assay (C) and the small-lawn slow killing assay (D). Each experiment contains 3–5 replicates of each condition (STAR Methods) for (C) and (D). The *nsy-1* and the *daf-2* mutant animals display decreased and increased resistance to PA14 infection (Garsin et al., 2003; Kim et al., 2002), respectively, in comparison with the naive wild-type animals, and serve as experimental controls. Kaplan-Meier procedure and log rank test.

(E) Although training with PA14 increases the expression of *lys-7p::gfp*, pheromone exposure further increases the expression in PA14-trained animals. One-way ANOVA with Tukey's multiple comparisons test. The fluorescence intensity of individual animals is normalized by the average fluorescence intensity of the naive animals; boxes show the median and first and third quartiles, and whiskers show the minimum and the maximum (GraphPad Prism 8). The numbers of the animals quantified are shown in the parentheses, and individual data points are shown as dots.

(F and G) A model for the function of INS-4 and INS-16 in regulating learning (F) and pheromone-mediated modulation of learning (G).

For (A)–(E), ****$p < 0.0001$, ***$p < 0.001$, **$p < 0.01$, and *$p < 0.05$; ns, not significant.

See also Figure S6.

AWA activity strongly reduced *ins-16* or *ins-4* expression in these two neurons, respectively (Figures 5H and 5I). Together our findings show that ADL and AWA neuronal activities critically regulate the expression of the two learning-regulating ILPs.

Pheromone Exposure Increases Feeding and Enhances Pathogen Resistance

If deleting both *ins-4* and *ins-16* does not affect the learning of the pathogenic PA14, what is the functional significance of expressing these two ILPs? Previous studies show that the high

worm density or the presence of high concentrations of the worm-secreted ascaroside pheromones promotes the formation of stress-resistant dauers (Butcher et al., 2008; Jeong et al., 2005; Kim et al., 2009). We found that cultivating the worms with a limited amount of food and the pheromone mixture (Figure S6; STAR Methods) strongly induced dauer formation in wild-type (Figure 6A). Although deleting *ins-4* alone did not alter dauer formation, deleting either *ins-16* alone or deleting both *ins-4* and *ins-16* significantly decreased dauer formation (Figure 6A). Thus, these ILPs also have functions in regulating dauer formation.

Learning to reduce the preference for pathogens, such as PA14, prevents the animals from eating harmful food. Without this learning ability, survival will be compromised unless animals also adopt alternative coping strategies. Thus, we hypothesized that, although social signals blocked the aversive learning, these signals likely promoted the consumption of the low-quality food, i.e., PA14, and the resistance to the pathogen. To test this hypothesis, we first measured the pumping rate, which indicated the rate of food intake (Avery and You, 2012). We found that training with the infectious bacterium PA14 significantly reduced the pumping rate, indicating a decreased food intake in the animals that learned to avoid PA14 (Figure 6B; STAR Methods). Interestingly, pheromone exposure increased the pumping rate of the PA14-trained animals on a PA14 lawn, as well as the pumping rate of the naive animals on OP50 (Figure 6B). These results demonstrate that the pheromone mixture that signals overcrowding promotes the consumption of food, including the consumption of the harmful food in trained animals. Because PA14 is infectious to the worms, we also tested whether pheromone exposure increased the resistance to PA14, which could mitigate the negative effects of eating the pathogen. Interestingly, using a slow-killing assay with a lawn of PA14 that either covered the whole plate or only covered the center of the plate (Reddy et al., 2009; Styer et al., 2008; Tan et al., 1999; STAR Methods), we found that the pheromones significantly improved the resistance to PA14 in both the naive animals and the trained animals (Figures 6C and 6D). In addition, the pheromone mixture significantly increased the expression of *lys-7* in trained animals, based on the signals of the *lys-7p::gfp* transcriptional reporter (Alper et al., 2007) in the pheromone-exposed and PA14-trained animals (Figure 6E). *lys-7* mediates innate immune responses to PA14 infection (Evans et al., 2008). Thus, these results indicate that pheromone exposure enhances the immune resistance to the infection of PA14. Together, we show that, during times of high population density, worms reprogram their physiological responses from learning to avoid bad food to increasing its consumption of and resistance against this harmful food.

DISCUSSION

The Pheromone Mixture that Signals Overcrowding Inhibits the Learning of Harmful Food

We examined whether the pheromone mixture that signals high-density conspecifics modulated a type of associative learning through which *C. elegans* learns to avoid the smell of bacteria food that makes them ill. We report that, when the population-density-signaling pheromones are abundant in the environment, the worms no longer learn to avoid the smell of the pathogenic bacteria. We show that the pheromones activate the sensory neuron ADL and increase its expression of the ILP *ins-16*. Increasing *ins-16* expression in ADL suppresses the sensory response of the bacteria-sensing neuron AWA and decreases its expression of *ins-4*, another ILP. Moreover, we show that learning requires a balance between the AWA-expressed INS-4 and the ADL-expressed INS-16, as well as the activities of ADL and AWA, which regulate the expression of *ins-16* and *ins-4*, respectively. Thus, disrupting the balance between INS-4 and INS-16 expression through pheromone-mediated sensory neuron activities inhibits learning (Figures 6F and 6G). Furthermore, we find that the pheromone mixture not only prevents the worms from learning to avoid the pathogenic bacteria, it also increases the ingestion of the harmful food and enhances the resistance to the pathogenic infection that likely becomes more severe as a result of ingesting more pathogenic bacteria. Together, we demonstrate how pheromones modulate a type of learning important in promoting worm survival and elucidate the molecular and cellular mechanisms that integrate social cues into the regulation of learning.

Our results demonstrate that learning depends on social context, which is among the most important conditions that impact survival. Previous studies show that pheromones that transmit social information between individual animals can either promote learning, such as the positive effect of darcin in mice on learning a location, or inhibit learning, such as the inhibitory effect of a pheromone produced by the queen honeybee on associative learning in young worker bees (Roberts et al., 2012; Vergoz et al., 2007). Our results on the modulatory effects of *C. elegans* pheromones that signal overcrowding on the olfactory learning, food intake, and immune resistance against the pathogenic food indicate that social pheromones regulate learning as part of a suite of adaptive traits generated in response to the signals of high population density. The set of behavioral and physiological adaptations together allows the worms to eat more pathogenic bacteria when a high density of conspecifics need to consume food. We suggest that our findings uncover a biological significance behind the diverse functions of the ILP family members in animal physiology: they contribute to the coordinated whole-organismic response to the environment.

AWA-Expressed *ins-4* and ADL-Expressed *ins-16* Regulate Learning and Mediate the Modulatory Effects of Social Pheromones on Learning

We show mechanistically that the social information represented by the pheromones modulates the learning of harmful food by regulating the ILPs in the sensory neurons ADL and AWA that respond to the pheromones and the food, respectively. Consistent with previous studies (Jang et al., 2012; Ryu et al., 2018), our results show that ADL respond to the ascaroside pheromones. We also find that training with PA14 decreases the response of ADL to the pheromones, suggesting a decreased repulsion of the pheromones to the worms after training. Prior pheromone exposure abolishes this training-dependent difference between naive and trained animals. In addition, although the AWA neurons in naive animals respond

to PA14 odorants as more attractive than OP50 odorants, training with PA14 reverses these sensory responses, demonstrating a decreased olfactory preference for PA14 in the trained animals. Pheromone exposure also significantly diminishes the difference in the AWA sensory response to PA14 between naive and trained animals. These results indicate that exposure to the pheromones modulates the sensory activities of ADL and AWA, both of which are required to generate and display normal learning. These results further show that ADL and AWA integrate the information of both social environment and food to modulate a food-seeking-related learning behavior.

ADL and AWA, respectively, produce the INS-16 and INS-4 signals to regulate learning. Pheromones activate ADL and increase *ins-16* expression, and increasing *ins-16* expression inhibits AWA sensory activity and the expression of *ins-4* in AWA. Furthermore, the activities of ADL and AWA regulate the expression of the ILPs that they produce. The regulation of gene transcription is a common cellular response to neuronal activity (Yap and Greenberg, 2018). Thus, the transcriptional regulation of the ILPs in response to the pheromone-dependent activities of the sensory neurons transduces social information into neuronal ILP signals that regulate learning of harmful food.

The insulin/ILP pathway functions widely in the brains of metazoans by acting through highly conserved receptors and intracellular kinase cascades. Multiple members of the insulin/ILP family are found in mammals, fruit flies, and worms to regulate physiological responses to various internal and external environments (Fernandes de Abreu et al., 2014; Fernandez and Torres-Alemán, 2012). Although mammalian insulin and ILPs exert their functions by binding to their own receptors with high affinity, the worm genome is so far known to encode a single insulin-like growth factor receptor DAF-2, which has been shown to produce at least two splice variants (Fernandez and Torres-Alemán, 2012; Kenyon et al., 1993; Kimura et al., 1997; Ohno et al., 2014). Thus, it is perhaps surprising to see that different ILPs in the worm play non-redundant functions and the ILPs produced by different neurons have distinct roles. For example, we have shown here that INS-4 produced by the AWA sensory neurons and INS-16 produced by the ADL sensory neurons regulate the learning of the pathogenic bacteria food. We propose that several mechanisms regulate the functional specificity of ILPs produced by different cells. Our results show that the neuronal activity of the sensory neurons regulates their production of the ILPs. Meanwhile, the release of neuropeptides, such as ILPs, is known to be strongly regulated by neuronal activity (van den Pol, 2012). In addition, the temporal pattern of extracellular signals, similar to those transmitted by ILPs, is critical for the biological responses elicited in the target cells (Ji et al., 2010). Thus, the production, release, and downstream effects of an ILP signal can be profoundly regulated by the activity of the neurons that generate it. We propose that the specific sensory-evoked activities in the pheromone-sensing ADL neurons and the food-sensing AWA neurons confer the functional specificity for the ADL-expressed INS-16 and the AWA-expressed INS-4, which are released with the appropriate temporal and spatial patterns to modulate learning. Functional specificity is also observed for mammalian ILPs generated by different sources, which likely represent specific information of distinct internal environments (Fernandez and Torres-Alemán, 2012). These findings together suggest that distinct functions of the ILP-producing neurons contribute to the functional specificity of the ILP family members, which carry different types of environmental information decoded by the releasing neurons. It is plausible that the production and release of many ILPs expressed in the nervous system will allow for the integration of various environmental information into the regulation of animal behavior and physiology.

The Balanced Expression of *ins-4* and *ins-16* Is Critical for Learning

The genetic interaction between *ins-4* and *ins-16* is intriguing. Although deleting either *ins-4* or *ins-16* disrupts learning, deleting both rescues the learning defect in the single mutants. Increasing the expression of either *ins-4* or *ins-16* also disrupts learning, revealing the critical role of the balanced expression of *ins-4* and *ins-16* in regulating learning. We propose that both *ins-4* and *ins-16* can inhibit learning and that they inhibit each other under a normal condition (Figures 6F and 6G). This model is consistent with the learning phenotypes of the single- and the double-mutant animals and with the modulatory effects of the social pheromones on learning. It is further supported by our findings that deleting *ins-16* or overexpressing *ins-16*, respectively, increases or decreases the expression of *ins-4* in AWA. However, *ins-4* does not suppress the expression of *ins-16*, suggesting that the inhibition of *ins-16* by *ins-4* likely occurs downstream of *ins-16* expression. This model represents the most likely scenario that explains how *ins-4* and *ins-16* regulate the olfactory learning of pathogenic bacteria and the pheromonal modulation of learning.

Several other studies reveal how ILP-to-ILP regulation contributes to the compensatory interactions between the ILP members and to their specific and diverse roles in the brain and other systems (Chen et al., 2013; Fernandes de Abreu et al., 2014; Fernandez and Torres-Alemán, 2012; Grönke et al., 2010). Here, we reveal a new type of signaling mechanism through which a balance between the INS-4 and INS-16 signals produced by specific sensory neurons is critical for their function in regulating olfactory learning of harmful food. Interestingly, both the social pheromones and the high-salt condition impinge on this exquisite ILP signaling mechanism to modulate the learning of the pathogenic food, revealing that ILPs act at the interface of environment and physiology to regulate adaptive responses to various internal and external conditions.

STAR★METHODS

Detailed methods are provided in the online version of this paper and include the following:

- KEY RESOURCES TABLE
- LEAD CONTACT AND MATERIALS AVAILABILITY
- EXPERIMENTAL MODEL AND SUBJECT DETAILS
- METHOD DETAILS
  - Transgenes and transgenic animals
  - Genotyping
  - Aversive olfactory training and two-choice olfactory preference assay
  - Confocal microscopy

SUPPLEMENTAL INFORMATION

Supplemental Information can be found online at https://doi.org/10.1016/j.neuron.2019.09.006.

ACKNOWLEDGMENTS

We thank the Caenorhabditis Genetics Center (funded by the NIH Office of Research Infrastructure P40 OD010440) for *C. elegans* strains; Martin Regenass and Iskra Katic at FMI for technical help; Dr. K. Kim for ADL::GCaMP3 transgenic strain; Dr. C. Bargmann for HisCl1 plasmids; and Drs. J. Kaplan and Y. Hao for help with constructing the miniMos transgenes. This work was supported by Novartis Research Foundation to J.A., ERC Starting Investigator Grant (NeuroAge 242666) and Research Councils UK Fellowship to Q.C., the NIH (GM118775) and National Science Foundation (Career 1555050) to R.A.B., and the NIH (GM108962, DC009852, and GM103770) to Y.Z.

AUTHOR CONTRIBUTIONS

Conceived Project, T.W. and Y.Z.; Designed Experiments, T.W., F.D., W.Y., H.L., and Y.Z.; Performed the Experiments, T.W., F.D., W.Y., H.L., A.C., D.A.F.d.A., A.R.D., Q.C., and J.A.; Interpreted Results, T.W. and Y.Z.; Wrote the Paper, T.W., J.A., Q.C., R.A.B., and Y.Z.

DECLARATION OF INTERESTS

The authors declare no competing interests.

Received: March 12, 2019
Revised: August 9, 2019
Accepted: September 6, 2019
Published: October 29, 2019

SUPPORTING CITATIONS

The following reference appears in the Supplemental Information: Hung et al. (2013).

REFERENCES

Alper, S., McBride, S.J., Lackford, B., Freedman, J.H., and Schwartz, D.A. (2007). Specificity and complexity of the Caenorhabditis elegans innate immune response. Mol. Cell Biol. *27*, 5544–5553.

Aguado, F., Sánchez-Franco, F., Rodrigo, J., Cacicedo, L., and Martínez-Murillo, R. (1994). Insulin-like growth factor I-immunoreactive peptide in adult human cerebellar Purkinje cells: co-localization with low-affinity nerve growth factor receptor. Neuroscience *59*, 641–650.

Alcedo, J., and Zhang, Y. (2013). Molecular and cellular circuits underlying Caenorhabditis elegans olfactory plasticity. In Invertebrate Learning and Memory, R. Menzel and P.R. Benjamin, eds. (Academic Press), pp. 112–123.

Avery, L., and You, Y.J. (2012). *C. elegans* feeding. In WormBook (The C. elegans Research Community). https://doi.org/10.1895/wormbook.1.150.1 http://www.wormbook.org/chapters/www_feeding/feeding.html.

Bargmann, C.I., Hartwieg, E., and Horvitz, H.R. (1993). Odorant-selective genes and neurons mediate olfaction in C. elegans. Cell *74*, 515–527.

Bredy, T.W., and Barad, M. (2008). Social modulation of associative fear learning by pheromone communication. Learn. Mem. *16*, 12–18.

Brenner, S. (1974). The genetics of Caenorhabditis elegans. Genetics *77*, 71–94.

Butcher, R.A., Fujita, M., Schroeder, F.C., and Clardy, J. (2007). Small-molecule pheromones that control dauer development in Caenorhabditis elegans. Nat. Chem. Biol. *3*, 420–422.

Butcher, R.A., Ragains, J.R., Kim, E., and Clardy, J. (2008). A potent dauer pheromone component in Caenorhabditis elegans that acts synergistically with other components. Proc. Natl. Acad. Sci. USA *105*, 14288–14292.

Butcher, R.A., Ragains, J.R., Li, W., Ruvkun, G., Clardy, J., and Mak, H.Y. (2009). Biosynthesis of the Caenorhabditis elegans dauer pheromone. Proc. Natl. Acad. Sci. USA *106*, 1875–1879.

Chabaud, M.A., Isabel, G., Kaiser, L., and Preat, T. (2009). Social facilitation of long-lasting memory retrieval in Drosophila. Curr. Biol. *19*, 1654–1659.

Chen, D., Katdare, A., and Lucas, N. (2006). Chemosignals of fear enhance cognitive performance in humans. Chem. Senses *31*, 415–423.

Chen, Z., Hendricks, M., Cornils, A., Maier, W., Alcedo, J., and Zhang, Y. (2013). Two insulin-like peptides antagonistically regulate aversive olfactory learning in C. elegans. Neuron *77*, 572–585.

Chronis, N., Zimmer, M., and Bargmann, C.I. (2007). Microfluidics for in vivo imaging of neuronal and behavioral activity in Caenorhabditis elegans. Nat. Methods *4*, 727–731.

Cornils, A., Gloeck, M., Chen, Z., Zhang, Y., and Alcedo, J. (2011). Specific insulin-like peptides encode sensory information to regulate distinct developmental processes. Development *138*, 1183–1193.

de Bono, M., and Maricq, A.V. (2005). Neuronal substrates of complex behaviors in C. elegans. Annu. Rev. Neurosci. *28*, 451–501.

Deijen, J.B., de Boer, H., and van der Veen, E.A. (1998). Cognitive changes during growth hormone replacement in adult men. Psychoneuroendocrinology *23*, 45–55.

Evans, E.A., Kawli, T., and Tan, M.W. (2008). Pseudomonas aeruginosa suppresses host immunity by activating the DAF-2 insulin-like signaling pathway in Caenorhabditis elegans. PLoS Pathog. *4*, e1000175.

Fernandes de Abreu, D.A., Caballero, A., Fardel, P., Stroustrup, N., Chen, Z., Lee, K., Keyes, W.D., Nash, Z.M., López-Moyado, I.F., Vaggi, F., et al. (2014). An insulin-to-insulin regulatory network orchestrates phenotypic specificity in development and physiology. PLoS Genet. *10*, e1004225.

Fernandez, A.M., and Torres-Alemán, I. (2012). The many faces of insulin-like peptide signalling in the brain. Nat. Rev. Neurosci. *13*, 225–239.

Frøkjær-Jensen, C., Davis, M.W., Sarov, M., Taylor, J., Flibotte, S., LaBella, M., Pozniakovsky, A., Moerman, D.G., and Jorgensen, E.M. (2014). Random and targeted transgene insertion in Caenorhabditis elegans using a modified Mos1 transposon. Nat. Methods *11*, 529–534.

Garcia, J., Kimeldorf, D.J., and Koelling, R.A. (1955). Conditioned aversion to saccharin resulting from exposure to gamma radiation. Science *122*, 157–158.

Garsin, D.A., Villanueva, J.M., Begun, J., Kim, D.H., Sifri, C.D., Calderwood, S.B., Ruvkun, G., and Ausubel, F.M. (2003). Long-lived C. elegans daf-2 mutants are resistant to bacterial pathogens. Science *300*, 1921.

Greene, J.S., Brown, M., Dobosiewicz, M., Ishida, I.G., Macosko, E.Z., Zhang, X., Butcher, R.A., Cline, D.J., McGrath, P.T., and Bargmann, C.I. (2016). Balancing selection shapes density-dependent foraging behaviour. Nature *539*, 254–258.

Grönke, S., Clarke, D.F., Broughton, S., Andrews, T.D., and Partridge, L. (2010). Molecular evolution and functional characterization of Drosophila insulin-like peptides. PLoS Genet. *6*, e1000857.

Guo, M., Wu, T.H., Song, Y.X., Ge, M.H., Su, C.M., Niu, W.P., Li, L.L., Xu, Z.J., Ge, C.L., Al-Mhanawi, M.T., et al. (2015). Reciprocal inhibition between sensory ASH and ASI neurons modulates nociception and avoidance in Caenorhabditis elegans. Nat. Commun. *6*, 5655.

Ha, H.I., Hendricks, M., Shen, Y., Gabel, C.V., Fang-Yen, C., Qin, Y., Colón-Ramos, D., Shen, K., Samuel, A.D., and Zhang, Y. (2010). Functional organization of a neural network for aversive olfactory learning in Caenorhabditis elegans. Neuron *68*, 1173–1186.

Han, S.K., Lee, D., Lee, H., Kim, D., Son, H.G., Yang, J.S., Lee, S.V., and Kim, S. (2016). OASIS 2: online application for survival analysis 2 with features for the analysis of maximal lifespan and healthspan in aging research. Oncotarget *7*, 56147–56152.

Hung, W.L., Hwang, C., Gao, S., Liao, E.H., Chitturi, J., Wang, Y., Li, H., Stigloher, C., Bessereau, J.L., and Zhen, M. (2013). Attenuation of insulin signalling contributes to FSN-1-mediated regulation of synapse development. EMBO J. *32*, 1745–1760.

Jang, H., Kim, K., Neal, S.J., Macosko, E., Kim, D., Butcher, R.A., Zeiger, D.M., Bargmann, C.I., and Sengupta, P. (2012). Neuromodulatory state and sex specify alternative behaviors through antagonistic synaptic pathways in C. elegans. Neuron *75*, 585–592.

Jeong, P.Y., Jung, M., Yim, Y.H., Kim, H., Park, M., Hong, E., Lee, W., Kim, Y.H., Kim, K., and Paik, Y.K. (2005). Chemical structure and biological activity of the Caenorhabditis elegans dauer-inducing pheromone. Nature *433*, 541–545.

Ji, Y., Lu, Y., Yang, F., Shen, W., Tang, T.T., Feng, L., Duan, S., and Lu, B. (2010). Acute and gradual increases in BDNF concentration elicit distinct signaling and functions in neurons. Nat. Neurosci. *13*, 302–309.

Jin, X., Pokala, N., and Bargmann, C.I. (2016). Distinct circuits for the formation and retrieval of an imprinted olfactory memory. Cell *164*, 632–643.

Karlson, P., and Luscher, M. (1959). Pheromones': a new term for a class of biologically active substances. Nature *183*, 55–56.

Kenyon, C., Chang, J., Gensch, E., Rudner, A., and Tabtiang, R. (1993). A C. elegans mutant that lives twice as long as wild type. Nature *366*, 461–464.

Kim, D.H., Feinbaum, R., Alloing, G., Emerson, F.E., Garsin, D.A., Inoue, H., Tanaka-Hino, M., Hisamoto, N., Matsumoto, K., Tan, M.W., and Ausubel, F.M. (2002). A conserved p38 MAP kinase pathway in Caenorhabditis elegans innate immunity. Science *297*, 623–626.

Kim, K., Sato, K., Shibuya, M., Zeiger, D.M., Butcher, R.A., Ragains, J.R., Clardy, J., Touhara, K., and Sengupta, P. (2009). Two chemoreceptors mediate developmental effects of dauer pheromone in C. elegans. Science *326*, 994–998.

Kimura, K.D., Tissenbaum, H.A., Liu, Y., and Ruvkun, G. (1997). daf-2, an insulin receptor-like gene that regulates longevity and diapause in Caenorhabditis elegans. Science *277*, 942–946.

Larsch, J., Flavell, S.W., Liu, Q., Gordus, A., Albrecht, D.R., and Bargmann, C.I. (2015). A circuit for gradient climbing in C. elegans chemotaxis. Cell Rep. *12*, 1748–1760.

Li, W., Kennedy, S.G., and Ruvkun, G. (2003). daf-28 encodes a C. elegans insulin superfamily member that is regulated by environmental cues and acts in the DAF-2 signaling pathway. Genes Dev. *17*, 844–858.

Liu, H., Yang, W., Wu, T., Duan, F., Soucy, E., Jin, X., and Zhang, Y. (2018). Cholinergic sensorimotor integration regulates olfactory steering. Neuron *97*, 390–405.e3.

Ludewig, A.H., Izrayelit, Y., Park, D., Malik, R.U., Zimmermann, A., Mahanti, P., Fox, B.W., Bethke, A., Doering, F., Riddle, D.L., and Schroeder, F.C. (2013). Pheromone sensing regulates Caenorhabditis elegans lifespan and stress resistance via the deacetylase SIR-2.1. Proc. Natl. Acad. Sci. USA *110*, 5522–5527.

Luo, L., Wen, Q., Ren, J., Hendricks, M., Gershow, M., Qin, Y., Greenwood, J., Soucy, E.R., Klein, M., Smith-Parker, H.K., et al. (2014). Dynamic encoding of perception, memory, and movement in a C. elegans chemotaxis circuit. Neuron *82*, 1115–1128.

Macosko, E.Z., Pokala, N., Feinberg, E.H., Chalasani, S.H., Butcher, R.A., Clardy, J., and Bargmann, C.I. (2009). A hub-and-spoke circuit drives pheromone attraction and social behaviour in C. elegans. Nature *458*, 1171–1175.

Marks, D.R., Tucker, K., Cavallin, M.A., Mast, T.G., and Fadool, D.A. (2009). Awake intranasal insulin delivery modifies protein complexes and alters memory, anxiety, and olfactory behaviors. J. Neurosci. *29*, 6734–6751.

McCarroll, S.A., Li, H., and Bargmann, C.I. (2005). Identification of transcriptional regulatory elements in chemosensory receptor genes by probabilistic segmentation. Curr. Biol. *15*, 347–352.

McGrath, P.T., Xu, Y., Ailion, M., Garrison, J.L., Butcher, R.A., and Bargmann, C.I. (2011). Parallel evolution of domesticated Caenorhabditis species targets pheromone receptor genes. Nature *477*, 321–325.

Mello, C.C., Kramer, J.M., Stinchcomb, D., and Ambros, V. (1991). Efficient gene transfer in C.elegans: extrachromosomal maintenance and integration of transforming sequences. EMBO J. *10*, 3959–3970.

Ohno, H., Kato, S., Naito, Y., Kunitomo, H., Tomioka, M., and Iino, Y. (2014). Role of synaptic phosphatidylinositol 3-kinase in a behavioral learning response in C. elegans. Science *345*, 313–317.

Pierce, S.B., Costa, M., Wisotzkey, R., Devadhar, S., Homburger, S.A., Buchman, A.R., Ferguson, K.C., Heller, J., Platt, D.M., Pasquinelli, A.A., et al. (2001). Regulation of DAF-2 receptor signaling by human insulin and ins-1, a member of the unusually large and diverse C. elegans insulin gene family. Genes Dev. *15*, 672–686.

Pokala, N., Liu, Q., Gordus, A., and Bargmann, C.I. (2014). Inducible and titratable silencing of Caenorhabditis elegans neurons in vivo with histamine-gated chloride channels. Proc. Natl. Acad. Sci. USA *111*, 2770–2775.

Reddy, K.C., Andersen, E.C., Kruglyak, L., and Kim, D.H. (2009). A polymorphism in npr-1 is a behavioral determinant of pathogen susceptibility in C. elegans. Science *323*, 382–384.

Ritter, A.D., Shen, Y., Fuxman Bass, J., Jeyaraj, S., Deplancke, B., Mukhopadhyay, A., Xu, J., Driscoll, M., Tissenbaum, H.A., and Walhout, A.J. (2013). Complex expression dynamics and robustness in C. elegans insulin networks. Genome Res. *23*, 954–965.

Roberts, S.A., Davidson, A.J., McLean, L., Beynon, R.J., and Hurst, J.L. (2012). Pheromonal induction of spatial learning in mice. Science *338*, 1462–1465.

Root, C.M., Ko, K.I., Jafari, A., and Wang, J.W. (2011). Presynaptic facilitation by neuropeptide signaling mediates odor-driven food search. Cell *145*, 133–144.

Ryu, L., Cheon, Y., Huh, Y.H., Pyo, S., Chinta, S., Choi, H., Butcher, R.A., and Kim, K. (2018). Feeding state regulates pheromone-mediated avoidance behavior via the insulin signaling pathway in *Caenorhabditis elegans*. EMBO J. *37*, e98402.

Sandberg, A.C., Engberg, C., Lake, M., von Holst, H., and Sara, V.R. (1988). The expression of insulin-like growth factor I and insulin-like growth factor II genes in the human fetal and adult brain and in glioma. Neurosci. Lett. *93*, 114–119.

Sarov, M., Schneider, S., Pozniakovski, A., Roguev, A., Ernst, S., Zhang, Y., Hyman, A.A., and Stewart, A.F. (2006). A recombineering pipeline for functional genomics applied to Caenorhabditis elegans. Nat. Methods *3*, 839–844.

Sengupta, P., Chou, J.H., and Bargmann, C.I. (1996). odr-10 encodes a seven transmembrane domain olfactory receptor required for responses to the odorant diacetyl. Cell *84*, 899–909.

Sokolowski, M.B. (2010). Social interactions in "simple" model systems. Neuron *65*, 780–794.

Srinivasan, J., Kaplan, F., Ajredini, R., Zachariah, C., Alborn, H.T., Teal, P.E., Malik, R.U., Edison, A.S., Sternberg, P.W., and Schroeder, F.C. (2008). A blend of small molecules regulates both mating and development in Caenorhabditis elegans. Nature *454*, 1115–1118.

Srinivasan, J., von Reuss, S.H., Bose, N., Zaslaver, A., Mahanti, P., Ho, M.C., O'Doherty, O.G., Edison, A.S., Sternberg, P.W., and Schroeder, F.C. (2012). A modular library of small molecule signals regulates social behaviors in Caenorhabditis elegans. PLoS Biol. *10*, e1001237.

Stiernagle, T. (2006). Maintenance of C. elegans. In WormBook (The C. elegans Research Community). https://doi.org/10.1895/wormbook.1.101.1 http://www.wormbook.org/chapters/www_strainmaintain/strainmaintain.html.

Styer, K.L., Singh, V., Macosko, E., Steele, S.E., Bargmann, C.I., and Aballay, A. (2008). Innate immunity in Caenorhabditis elegans is regulated by neurons expressing NPR-1/GPCR. Science *322*, 460–464.

Stylianopoulou, F., Herbert, J., Soares, M.B., and Efstratiadis, A. (1988). Expression of the insulin-like growth factor II gene in the choroid plexus and the leptomeninges of the adult rat central nervous system. Proc. Natl. Acad. Sci. USA *85*, 141–145.

Tan, M.W., Mahajan-Miklos, S., and Ausubel, F.M. (1999). Killing of Caenorhabditis elegans by Pseudomonas aeruginosa used to model mammalian bacterial pathogenesis. Proc. Natl. Acad. Sci. USA *96*, 715–720.

Tomioka, M., Adachi, T., Suzuki, H., Kunitomo, H., Schafer, W.R., and Iino, Y. (2006). The insulin/PI 3-kinase pathway regulates salt chemotaxis learning in Caenorhabditis elegans. Neuron *51*, 613–625.

van den Pol, A.N. (2012). Neuropeptide transmission in brain circuits. Neuron *76*, 98–115.

Vergoz, V., Schreurs, H.A., and Mercer, A.R. (2007). Queen pheromone blocks aversive learning in young worker bees. Science *317*, 384–386.

White, J.G., Southgate, E., Thomson, J.N., and Brenner, S. (1986). The structure of the nervous system of the nematode Caenorhabditis elegans. Philos. Trans. R. Soc. Lond. B Biol. Sci. *314*, 1–340.

Wu, Q., Zhao, Z., and Shen, P. (2005). Regulation of aversion to noxious food by Drosophila neuropeptide Y- and insulin-like systems. Nat. Neurosci. *8*, 1350–1355.

Yamada, K., Hirotsu, T., Matsuki, M., Butcher, R.A., Tomioka, M., Ishihara, T., Clardy, J., Kunitomo, H., and Iino, Y. (2010). Olfactory plasticity is regulated by pheromonal signaling in Caenorhabditis elegans. Science *329*, 1647–1650.

Yap, E.L., and Greenberg, M.E. (2018). Activity-regulated transcription: bridging the gap between neural activity and behavior. Neuron *100*, 330–348.

Zaslaver, A., Liani, I., Shtangel, O., Ginzburg, S., Yee, L., and Sternberg, P.W. (2015). Hierarchical sparse coding in the sensory system of Caenorhabditis elegans. Proc. Natl. Acad. Sci. USA *112*, 1185–1189.

Zhang, Y., Lu, H., and Bargmann, C.I. (2005). Pathogenic bacteria induce aversive olfactory learning in Caenorhabditis elegans. Nature *438*, 179–184.

STAR★METHODS

KEY RESOURCES TABLE

REAGENT or RESOURCE	IDENTIFIER	SOURCE
Bacteria or Ascarosides		
Pseudomonas aeruginosa PA14	PA14	Kim et al. (2002)
Escherichia coli OP50	OP50	*Caenorhabditis* Genetics Center (CGC)
Ascaroside #2	asc-C6-MK; C6	Butcher et al. (2007, 2008, 2009)
Ascaroside #3	asc-ΔC9; C9	Butcher et al. (2007, 2008, 2009)
Ascaroside #5	asc-ωC3; C3	Butcher et al. (2007, 2008, 2009)
Histamine- dihydrochloride		Sigma-Aldrich
Experimental Models: Organisms/Strains		
Wild type	N2(Bristol)	CGC
daf-22(m130) II	DR476	CGC
ins-2(tm4467) II	QL76	Fernandes de Abreu et al., 2014
ins-3(tm3608) II	QL28	Fernandes de Abreu et al., 2014
ins-4(tm3620) II	QL27	Fernandes de Abreu et al., 2014
ins-5(tm2560) II	QL24	Fernandes de Abreu et al., 2014
ins-8(tm4144) IV	QL52	Fernandes de Abreu et al., 2014
ins-16(ok2919) III	QL53	Fernandes de Abreu et al., 2014
ins-22(ok3616) III	QL46	Fernandes de Abreu et al., 2014
ins-23(tm1875) III	QL14	Fernandes de Abreu et al., 2014
ins-25(ok2773) I	QL47	Fernandes de Abreu et al., 2014
ins-28(ok2722) I	QL48	Fernandes de Abreu et al., 2014
ins-33(tm2988) I	QL50	Fernandes de Abreu et al., 2014
ins-35(ok3297) V	QL51	Fernandes de Abreu et al., 2014
ins-39(tm6467) X	ZC2751	This study
daf-2(e1368) III	QZ120	Chen et al., 2013
kyIs140 I; nsy-1(ky397) II	CX4998	CGC
ins-4(tm3620) II; ins-16(ok2919) III	ZC2825	This study
hpDf761 II; unc-119(ed3) III	ZM6523	Hung et al., 2013
ins-4(tm3620) II; ins-7(tm2001) IV	ZC2746	This study
ins-6(tm2416) II; ins-16(ok2919) III	ZC2826	This study
ins-16(ok2919) III; ins-7(tm2001) IV	ZC2827	This study
ins-16(ok2919) III; daf-2(e1368) III	ZC3190	This study
ins-4(tm3620) II; daf-2(e1368) III	ZC3192	This study
ins-4(tm3620) II; ins-16(ok2919) III; daf-2(e1368) III	ZC3248	This study
ins-4(tm3620) II; yxEx1434[ins-4p::ins-4::3′UTR; unc-122p::gfp]	ZC2772	This study
ins-4(tm3620) II; yxEx1461[odr-10p::ins-4; unc-122p::gfp]	ZC2835	This study
ins-4(tm3620) II; yxEx1618[gpa-4p::ins-4; unc-122p::gfp]	ZC3120	This study
ins-4(tm3620) II; yxEx1555[gcy-36p::ins-4; unc-122p::gfp]	ZC3009	This study
ins-16(ok2919) III; yxEx1442 [ins-16p::ins-16::3′UTR; unc-122p::gfp]	ZC2792	This study
ins-16(ok2919) III; yxEx1480[srh-220p::ins-16; unc-122p::gfp]	ZC2863	This study
jxSi27[ins-4p::mCherry] II	QZ716	This study
drcSi63[ins-16p::mCherry] II	QL263	This study
jxSi27 II; yxEx1455[odr-10p::gfp; unc-122p::gfp]	ZC2821	This study
drcSi63 II; yxEx1468[srh-220p::gfp; unc-122p::gfp]	ZC2845	This study

(*Continued on next page*)

Continued

REAGENT or RESOURCE	IDENTIFIER	SOURCE
yxSi1[odr-10p::ins-4] X	ZC2969	This study
ins-4(tm3620) II; ins-16(ok2919) III; yxSi6[odr-10p::ins-4] I	ZC2996	This study
yxSi8[ins-16p::ins-16] I	ZC3089	This study
ins-4(tm3620) II; ins-16(ok2919) III; yxSi10[ins-16p::ins-16] I	ZC3091	This study
yxSi8 I; yxSi1 X	ZC3260	This study
lskEx218[sre-1p::GCaMP3; unc-122p:dsRed]	KHK225	Ryu et al., 2018
yxEx1393[gpa-4delta6p::GCaMP6s; unc-122p::dsRed2]	ZC2706	This study
jxSi27 II; yxEx1582[gpa-4p::gfp; unc-122p::gfp]	ZC3037	This study
jxSi27 II; yxEx1552[gcy-36p::gfp; unc-122p::gfp]	ZC3006	This study
yxEx1638[odr-10p::HisCl1; unc-122p::gfp]	ZC3160	This study
yxEx1683[srh-220p::HisCl1; unc-122p::gfp]	ZC3237	This study
yxSi8 I; jxSi27 II	ZC3186	This study
jxSi27 II; ins-16(ok2919) III	ZC2893	This study
ins-4(tm3620) II; drcSi63 II	ZC3187	This study
ins-16(ok2919) III; yxEx1393	ZC2896	This study
yxSi8 I; yxEx1393	ZC3188	This study
jxSi27 II; yxEx1638	ZC3261	This study
drcSi63 II; yxEx1683	ZC3264	This study
pha-1(e2123) III; denEx2	SAL105	Alper et al., 2007
Software		
GraphPad Prism 8	https://www.graphpad.com	
Igor Pro 6.12	https://www.wavemetrics.com	
Fiji/ImageJ	https://fiji.sc/	

LEAD CONTACT AND MATERIALS AVAILABILITY

Further information and requests for resources and reagents should be directed to and will be fulfilled by the Lead Contact, Yun Zhang (yzhang@oeb.harvard.edu).

All unique/stable reagents generated in this study are available from the Lead Contact without restriction.

EXPERIMENTAL MODEL AND SUBJECT DETAILS

The *Caenorhabditis elegans* hermaphrodites were used in this study. The *C. elegans* strains were maintained at 20°C as described (Brenner, 1974). The strains used in this study are listed in the Key Resources Table.

METHOD DETAILS

Transgenes and transgenic animals

To make the DNA plasmid *ins-4p::ins-4::3′UTR*, a 4 kb DNA fragment was generated using polymerase chain reaction (PCR) (forward primer 5′ agagttgtcaagaagtgcgtcaagttgt 3′ and reverse primer 5′ gacaaccgtccctccgtttcataataa 3′) and cloned into the pCR8 Gateway entry vector (Invitrogen). To make the DNA plasmid *ins-16p::ins-16::3′UTR*, a 4.7 kb DNA fragment was generated using PCR (forward primer 5′ gttgagggctatatcttgtaaacagacag 3′ and reverse primer 5′ aagtctgaagtttagccaaggttgagccta 3′) and cloned into the pCR8 Gateway entry vector (Invitrogen). To make *ins-4p::mCherry*, we used recombineering pipeline (Sarov et al., 2006) to replace the *ins-4* coding sequence on WEM061CG10 fosmid with *mCherry* cassette generated by PCR (ins-4 Redplf Fw: 5′ tgttaattttcataatttttcagaagtttttcaaaagctccaagagaatgAGCTCAGGAGGTAGCGG 3′ and ins-4 Redplf Rv: 5′ ctctattgaaaattatttgacgac ggagatggcttgttggacgactgtttGGCAGATCGTCAG TCAG 3′) and subcloned the *ins-4::mCherry* fusion into the BSD vector generated with PCR (5′ tttacctcaattttccagactcaatcgaaactcttcaatcttcaaggaaacctaggTTAGCCCTCCCACACATAACC 3′ and ins-4 PUBp15A: 5′ gtccaatataaaacgagtcttgacacatttatcaattcctgttctgaatacctgcaggCTAGGGAT AACAGGGTAATTG 3′) and then cloned into vectors for MosSCI to integrate the reporter at the ttTI5605 site on LGII. To make *ins-16p::mCherry*, the *ins-16* 5′ intergenic sequence (16 5UTR Rv: 5′ atcgctcgagtgtaaaagtgattttgaaaatt 3′, 16 5UTR Fw: 5′ ataagatctcctgtaaatttttgttttagag 3′), *ins-16* 3′ intergenic sequence (16 3UTR Fw 2: 5′ tcaaggcgcgcctatcaaaattgttatttatttttgttaatttgttaataaatattatatttagtcatg 3′, 16 3UTR Rv 2: 5′ ctaacctgcagg

aataaggactgggtagttgaaagtcagaaaaagcaagagc 3′) and mCherry (36_16mcherry Fw: 5′ cgccctcgagaATGAGCTCAGGAGGTAGC GGC 3′, 16mCherry Rv: 5′ taacctgcaggaggcgcgccaGGCAGATCGTCAGTCAGGAAGTTC 3′) were made by PCR with the respective primers that added restriction sites for cloning into a MosSCI vector to integrate the reporter at the ttTI5605 site on LGII. To make the DNA plasmid *odr-10p::ins-4::unc-54 3′UTR*, a 1.22 kb DNA sequence upstream of the *odr-10* gene expressed specifically in the sensory neuron AWA (Sengupta et al., 1996) was generated using PCR, cloned into the pCR8 Gateway entry vector (Invitrogen) and recombined with the destination vector *pDEST-ins-4::unc-54 3′UTR* by following the manufacturer's guidelines. To make *pDEST-ins-4::unc-54 3′UTR,* the coding and 3′ untranslated region of the *ins-4* genomic locus (634bp) was amplified from wild-type genomic DNA (NheI_ins-4_primer_F: 5′ CGGCTAGCAGAAGTTTTTCAAAAGC 3′ and KpnI_ins-4_primer_R: 5′ CCGGTACCAT TCAAAAAGTTTTATTGCAG 3′) and cloned into a pDEST vector. A 2.46 kb *gpa-4* promoter and a 1.09 kb *gcy-36* promoter were used for expression in ASI and URX, respectively (Chen et al., 2013; Guo et al., 2015). To generate the plasmid *srh-220p::ins-16::unc-54 3′UTR*, a 4 kb DNA sequence upstream of the *srh-220* gene specifically expressed in the ADL (McCarroll et al., 2005) was generated using PCR, cloned into the pCR8 Gateway entry vector and recombined with the *pDEST-ins-16::unc-54 3′UTR* following the manufacture's instruction. To make *pDEST-ins-16::unc-54 3′UTR*, the coding region of the *ins-16* genomic locus (285bp) was amplified from wild-type genomic DNA (NheI_ins-16_primer_F: 5′ CGGCTAGCATGCAAAGCCTA 3′ and KpnI_ins-16_primer_R: 5′ CCGGTACCTTAAATTTTGTCGATT 3′) and cloned into a pDEST vector. To make *pDEST-HisCl1::unc-54 3′UTR*, the coding region of HisCl1 was digested from pNP403 (gift from Dr. C. Bargmann) by using NheI and KpnI and cloned into a pDEST vector. Transgenic animals were generated by injecting transgene(s) (10 - 30 ng/μL) mixed with a co-injection marker *unc-122p::gfp* or *unc-122p::DsRed2* (10 ng/μL) using the standard methods (Mello et al., 1991). The transgenic animals containing single-copy transgenes, *yxSi1[odr-10p::ins-4]*, *yxSi6[odr-10p::ins-4], yxSi8[ins-16p::ins-16]*, or *yxSi10[ins-16p::ins-16]* were generated and isolated with the miniMos method (Frøkjær-Jensen et al., 2014).

Genotyping

Two pairs of primers were designed to examine the genotype of *ins-4((tm3620)* or *ins-16(ok2919)* using PCR. One pair differentially amplifies wild-type and mutant isoforms of each gene, while the other pair only amplifies the corresponding wild-type sequence. The primers are: for *ins-4(tm3620),* 5′ gatgtgacctccagatgaact 3′, 5′ gatggcttgttggacgactg 3′; 5′ gatgtgacctccagatgaact 3′, 5′ catggttct ccacaggttgac 3′; for *ins-16(ok2919)*, 5′ gtctgaaccttggtcaagca 3′, 5′ ggaaaatttcaatttcggca 3′; 5′ gtctgaaccttggtcaagca 3′, 5′ gc aactgttgtagcctacc 3′. The DNA fragments generated by PCR were sequenced to confirm the deletions. The flanking regions and the deletions are: *ins-4(tm3620)* 5′ accttccatggacaccagcaaa [153bp deletion] acgtttaatgctaaaaattttt 3′; *ins-16(ok2919)* 5′ cggaaaattt caatttcggcaa [438bp deletion] ccgggagctcaaacgttgttct 3′.

Aversive olfactory training and two-choice olfactory preference assay

The long-term aversive olfactory training and the two-choice olfactory preference assay were performed similarly as described previously (Chen et al., 2013) and as shown in Figure 1A. To prepare a training plate, 250 μL PA14 culture in NGM medium (nematode growth medium, 2.5 g peptone/L, 3.0 g NaCl/L, 1 mM CaCl2, 1 mM MgSO4, 25 mM KPO4 pH 6.0, 1 mL 5 mg/mL Cholesterol/L) generated by incubation at 26°C overnight was spread on one side of a 10 cm NGM plate and 50 μL OP50 culture in NGM medium similarly prepared was spread on the side of the PA14 lawn (Figure 1A). To make a control naive plate, 250 μL OP50 culture was spread on a 10 cm NGM plate. The plates were dried on bench, incubated at 26°C for 36 hours and cooled down to room temperature before use. Embryos were collected by bleaching well-staged and well-fed gravid adults cultivated under the standard condition. Around 500 embryos were put on each naive or training plate for training. The standard chemotaxis plates (1 mM CaCl2, 1 mM MgSO4, 5 mM KPO4 pH6.0) were used for assay. To prepare the bacteria spots for the choice assay, a single OP50 or PA14 colony was picked into 30 mL NGM medium in a 250 mL flask to incubate at 26°C overnight to reach the OD_{600} between 0.3 and 0.5 for OP50 culture and between 0.5 to 0.7 for PA14 culture. The culture was span down in a benchtop centrifuge at 4,000 rpm for 15 minutes, the supernatant was removed and the bacteria pellets were resuspended with NGM medium to reach final OD_{600} around 1.0. Twenty-five μL of resuspended bacteria culture of OP50 or PA14 was added to the two opposite sides of an assay plate, air-dried and let stand at room temperature for less than 2 hours before use. Animals were washed off from the training plate or the control plate and washed twice before putting on the assay plate. 50-200 worms were put in the center of each assay plate, dried with Kimwipse and assayed for 90 minutes. At the end of the assay, 1 μL 1M sodium azide was added to each bacterial lawn to immobilize the worms for counting. A choice index was determined as the number of the worms on the small OP50 lawn minus the number of the worms on the small PA14 lawn, which was normalized by the total number of the worms in one assay. A learning index was determined as the choice index of one assay on the trained animals subtracted by the average choice index of the naive animals on the day, similarly as previously described (Jin et al., 2016). A positive choice index indicates a preference for OP50 and a positive learning index indicates learned avoidance of PA14.

In all pheromone experiments a 1:1:1 ratio of three ascarosides, ascr#2 (asc-C6-MK; C6), ascr#3 (asc-ΔC9; C9), and ascr#5 (asc-ωC3; C3) (Butcher et al., 2007, 2008), was used to reach a final concentration of 1 μM for each. Briefly, the appropriate amount of ascaroside stock solution made with 200 proof ethanol (33.3 μL of a 3mM stock of each ascaroside) was added to 100 mL NGM agar that had cooled to ~55°C to reach the final concentration. The plates were stored at 4°C and used within one week. The NGM plates and the assay plates with 50mM or 200mM NaCl were made similarly as described above with the appropriate NaCl concentration. The training and the assays under the high salt condition were performed similarly as described above. To inhibit

neurons that expressed HisCl1, histamine-dihydrochloride (Sigma-Aldrich) was added to the NGM plates and/or the assay plates as needed to reach a final concentration of 5 mM. The training and assay were otherwise performed as described above. The statistical analyses were done using GraphPad Prism 8.

Confocal microscopy

Images were collected on a confocal Nikon Eclipse Ti-E inverted microscope with a 40x oil-immersion objective with an ANODR iXon Ultra EMCCD camera. NIH ImageJ was used to generate a maximum intensity Z-projection. The intensity of a reporter expression in each cell body was determined as the mean value of a circle centered on the soma minus the mean background intensity. The expression intensities of multiple somata were measured on different days. Adult worms were used for the quantitation. The statistical analyses were done using GraphPad Prism 8.

Calcium imaging

Calcium imaging was performed essentially as previously described (Ha et al., 2010) using a microfluidic device that delivered the stimulants and limited the movement of the animal (Chronis et al., 2007). The animals were cultivated and treated with pheromones as described above. To prepare the bacteria-conditioned media, a single OP50 or PA14 colony was picked into 30 mL NGM medium in a 250 mL flask to incubate at 26°C overnight to reach the OD_{600} between 0.3 and 0.5 for OP50 culture and between 0.5 to 0.7 for PA14 culture. The culture was span down in a benchtop centrifuge at 4,000 rpm for 15 minutes and the supernatant was collected to use as the conditioned-medium. To prepare the pheromones for imaging, 3.3 μL stock solution of C3, C6 and C9 at 3 mM each was added into 10 mL NGM buffer to reach the final concentration of each ascaroside at 1 μM. The movies for the fluorescence time-lapse imaging were collected using a Nikon Eclipse Ti-U inverted microscope with a 40X oil immersion objective equipped with a Yokogawa CSU-X1 scanner unit and a Photometrics CoolSnap EZ camera at 5 frames per second. The movies were analyzed by using Fiji. Briefly, the GCaMP signal of the imaged neuron on each movie frame, *F,* was determined as the average fluorescence intensity of a region of interest (ROI) that contained the soma of the neuron subtracted by the average fluorescence intensity of the background of the same size and shape. $F_{baseline}$ is the average fluorescence intensity during the 30 s window before the PA14 stimulation or the pheromone stimulation and $(F - F_{baseline})/F_{baseline}$ *(%)* was obtained for all frames in each movie. Multiple worms were imaged for each experiment and average $(F - F_{baseline})/F_{baseline}$ *(%)* were plotted as a function of time.

Measuring dauer formation

The assay plates were prepared one day before use. 500 mL NGM-agar (no peptone) was autoclaved and cooled down to 55°C. The pheromone mixture was added to the NGM-agar to make the final concentration of each ascaroside to be 1 μM (aliquot 3 mL NGM-agar and 50 μL diluted pheromone mixture containing 1 μL 3 mM C3, 1 μL 3 mM C6, 1 μL 3 mM C9 and 47 μL water to each 3.5 cm assay plate). To prepare the OP50 food, an individual OP50 colony was picked into 30 mL Luria Broth (LB) in a 50 mL falcon tube and incubated at 26°C overnight to reach the OD_{600} between 0.6 and 0.8. The OP50 culture was span down in a benchtop centrifuge at 4,000 rpm for 15 minutes, supernatant was removed and the bacteria pellet was resuspended with 3 mL LB. Twenty μL resuspended OP50 was added to the center of an assay plate and dried close to a flame. Five young adult worms were picked onto each assay plate to lay eggs for about 3 hours and then removed. The assay plate was placed in a closed plastic box containing a damp paper towel, which was put in a 25°C incubator for about 64-72 hours before the numbers of dauers and L4/adults on each plate were counted. The percent of offspring dauer was quantified by dividing the number of dauers on each plate by the total number of dauers plus L4/adults. The dauer index was calculated as (percent of offspring dauer) / (average percent of wild-type offspring dauer) x 100%. The statistical analyses were done using GraphPad Prism 8.

Measuring pumping rate

The pumping rate under each condition was measured on the third day of the training (Figures 1A and 1B). The pharyngeal pumps in each worm were counted under Zeiss AXIO Zoom V16 microscope for 3 times and for 20 s each time, the total number of which generated the pumping rate (pumps/minute) for the animal. The statistical analyses were done using GraphPad Prism 8.

Slow killing assay

The slow killing assay was performed similarly as described (Reddy et al., 2009; Styer et al., 2008; Tan et al., 1999). To make a plate for the slow killing assay with a full lawn, 100 μL overnight LB culture of PA14 was spread on a 6 cm NGM plate to cover the plate completely. To make a plate for the slow killing assay with a small lawn, 10 μL PA14 was put on the center of a 3.5 cm NGM plate. The seeded plates were incubated at 37°C for 24 hours and then at 25°C for overnight to grow the PA14 lawns. Twenty to thirty adult animals from the naive plate, the training plate, the naive plate containing the pheromones, or the training plate containing the pheromones were transferred onto each slow killing assay plate. All of the assay plates were kept at 25°C and scored for live and dead worms twice every day or as frequently as needed. Live worms were transferred to fresh slow killing assay plates on each day to prevent confusion between the tested animals and their progeny. No DNA synthesis inhibitor or RNAi treatment was used during the assay. The statistical analyses were done using GraphPad Prism 8 and OASIS 2 (Han et al., 2016).

Liquid culture of *C. elegans* in high density

The liquid culture of *C. elegans* was generated as described previously (Stiernagle, 2006). Briefly, 75 mL S Medium (to make 1L S Medium, 1L S Basal, 10 mL trace metals solution, 10 mL 1 M potassium citrate, 3 mL 1 M $MgSO_4$, 3 mL 1 M $CaCl_2$ were mixed together with all components sterilized with appropriate filters) was added to a sterilized 500 mL flask and inoculated with concentrated *E. coli* OP50. Adult worms were bleached and the eggs were washed with 1 mL M9 buffer for twice. The eggs were added to the 75 mL S Medium in the flask, which was put on a shaker at 120 rpm at 20°C for 6 days. Concentrated *E. coli* OP50 suspended in S Medium was added daily to provide a sufficient amount of food. The culture was transferred to a 50 mL sterile conical centrifuge tube and spun down by using a benchtop centrifuge at 4,000 rpm for 15 minutes. The supernatant was filtered three times. Fifty mL of the filtered supernatant or 50 mL S Medium was added into 250 mL NGM agar to make training or naive plates. The training and the assay were performed similarly as described above.

QUANTIFICATION AND STATISTICAL ANALYSIS

The boxplots were generated using Igor Pro 6.12 or GraphPad Prism 8, the statistical tests were performed using GraphPad Prism 8, and imaging analysis was done using Fiji or ImageJ. The statistical tests, value of n and what each n value represents, and other related measures are shown in the legend of each relevant figure. In all, **** $p < 0.0001$, *** $p < 0.001$, ** $p < 0.01$, * $p < 0.05$, ns, not significant.

DATA AND CODE AVAILABILITY

The published article includes all datasets generated or analyzed during this study.